J|A|C|S ARTICLES

Published on Web 07/06/2009

High-Field EPR and Magnetic Susceptibility Studies on Binuclear and Tetranuclear Copper Trifluoroacetate Complexes. X-ray Structure Determination of Three Tetranuclear Quinoline Adducts of Copper(II) Trifluoroacetate

Andrew Ozarowski,*,† Iwona B. Szymańska,‡ Tadeusz Muzioł,‡ and Julia Jezierska§

National High Magnetic Field Laboratory, Florida State University, 1800 East Paul Dirac Drive, Tallahassee, Florida 32310, Department of Chemistry, Nicolaus Copernicus University, ul. Gagarina 7, Toruń 87100, Poland, and Faculty of Chemistry, Wrocław University, ul. F. Joliot-Curie 14, Wrocław 50383, Poland

Received April 3, 2009; E-mail: ozarowsk@magnet.fsu.edu

Abstract: Magnetic properties and high-field EPR spectra of three previously unknown tetranuclear quinoline adducts of copper(II) trifluoroacetate were studied, and their X-ray structures were determined. Two green complexes containing a μ_4-oxo bridge, $Cu_4O(CF_3COO)_6(quin)_4\cdot(C_6H_5CH_3)_{0.6}$ (orthorhombic, *Pbca*, a = 15.278(3), b = 23.227(5), c = 34.895(7) Å) and $Cu_4O(CF_3COO)_6(quin)_4\cdot(C_6H_6)_{0.8}$ (monoclinic, *P*2/*c*, a = 21.933(4), b = 11.176(2), c = 23.927(5) Å, β = 97.41(3)°) are ferromagnetic, whereas the blue complex $[Cu_4(OH)_2(CF_3COO)_8(quin)_2]^{2-}(quinH^+)_2$ (monoclinic, a = 21.933(4), b = 11.176(2), c = 23.927(5) Å, β = 97.41(3)°), formed in humid air from the solid dimeric $[Cu(CF_3COO)_2\cdot(quin)]_2$, is antiferromagnetic, as is the tetranuclear blue product formed in humid air of the μ_4-oxo tetramers. High-field EPR spectra allowed determination of the spin Hamiltonian parameters for the spin quintet state (S = 2) in the ferromagnetic complexes, which facilitated accurate interpretation of their magnetic susceptibility data. "Broken symmetry" DFT calculations were performed to estimate the exchange integrals in all three tetranuclear complexes, showing surprisingly good agreement with experimental results. Negative sign of the zero-field splitting parameter D in two binuclear complexes, $[Cu(CF_3COO)_2\cdot CH_3CN]_2$ and $[Cu(CF_3COO)_2\cdot(quin)]_2$, was found from single-crystal high-field EPR spectra, confirming recent results for nonhalogenated dimeric copper carboxylates.

Introduction

Binuclear and polynuclear copper carboxylates have been subject to extensive experimental and theoretical studies ever since Bleaney and Bowers discovered intramolecular antiferromagnetic interactions in binuclear copper acetate monohydrate.[1] Factors affecting the magnitude and character of the exchange interactions in bridged binuclear transition metal complexes have been of particular interest.[2,3]

Dimeric "paddlewheel" structures are very conspicuous among copper(II) complexes of formic acid and its homologues,[3] while such arrangements are much less numerous in the case of the perfluorinated carboxylic acids, which tend to form either monomeric copper complexes or more extended chains.[4] Dimeric paddlewheel adducts $[Cu(CF_3COO)_2\cdot(CH_3CN)]_2$[5] and $[Cu(CF_3COO)_2\cdot(quin)]_2$[6] (quin = quinoline) are rare exceptions. Copper(I) and copper(II) perfluorocarboxylates are volatile, which makes them potentially useful in the chemical vapor deposition technique to produce thin metallic copper layers,[7] and from that viewpoint the determination of nuclearity of such complexes is very important. Magnetic susceptibility measurements and electron paramagnetic resonance are methods of choice to accomplish this task. In this way, these complexes are on the crossroads of pure and applied chemistry and offer an opportunity of investigating the metal−metal interactions in systems substantially different from the better-known nonhalogenated copper carboxylates. One of us has recently[8] investigated by high-field EPR the zero-field splitting in copper acetate monohydrate and its pyrazinate adduct to find that the zero-field splitting parameter D is negative. $|D|$ in $[Cu(CF_3COO)_2(quin)]_2$ has been reported to be substantially larger than in simple copper carboxylates,[6] and this research was undertaken in part to determine whether D carries a negative sign in the trifluoroacetate copper complexes as well.

In the course of this work we encountered the surprisingly rich system Cu(II)-trifluoroacetate-quinoline. In addition to the

† Florida State University.
‡ Nicolaus Copernicus University.
§ Wrocław University.

(1) Bleaney, B.; Bowers, K. D. *Proc. R. Soc. A* **1952**, *214*, 451–465.
(2) Hay, P. J.; Thibeault, J. C.; Hoffmann, R. *J. Am. Chem. Soc.* **1975**, *97*, 4884–4899.
(3) Melnik, M. *Coord. Chem. Rev.* **1981**, *36*, 1–44.
(4) Cotton, F. A.; Dikarev, E. V.; Petrukhina, M. A. *Inorg. Chem.* **2000**, *39*, 6072–6079.
(5) Karpova, E. V.; Boltalin, A. I.; Zakharov, M. A.; Sorokina, N. I.; Korenev, Yu. M.; Troyanov, S. I. Z. *Anorg. Allg. Chem.* **1998**, *624*, 741–744.
(6) Moreland, J. A.; Doedens, R. J. *J. Am. Chem. Soc.* **1975**, *97*, 508–513.
(7) Grodzicki, A.; Lakomska, I.; Piszczek, P.; Szymanska, I.; Szlyk, E. *Coord. Chem. Rev.* **2005**, *249*, 2232–2258.
(8) Ozarowski, A. *Inorg. Chem.* **2008**, *47*, 9760–9762.

dimer mentioned above, two green ferromagnetic tetranuclear complexes $Cu_4O(CF_3COO)_6(quin)_4\cdot(C_6H_5CH_3)_{0.6}$ and $Cu_4O(CF_3COO)_6(quin)_4\cdot(C_6H_6)_{0.8}$ were synthesized, and their structures were determined. A blue product formed from the tetranuclear complexes on exposure to humid air was also found to be tetranuclear but antiferromagnetic. Also, the blue antiferromagnetic complex $[Cu_4(OH)_2(CF_3COO)_8(quin)_2]^{2-}(quinH^+)_2$ formed from $[Cu(CF_3COO)_2(quin)]_2$ on exposure to humid air was found to be tetrameric, and its X-ray structure was resolved.

Experimental Section

The X-band EPR spectra were recorded on a Bruker ElexSys spectrometer (Bruker, Germany). High-frequency EPR spectra at temperatures ranging from ca. 3 to 290 K were recorded on a home-built spectrometer at the EMR facility of NHMFL.[9] The instrument was a transmission-type device in which microwaves are propagated in cylindrical lightpipes. The microwaves were generated by a phase-locked Virginia Diodes source generating a frequency of 13 $\pm$ 1 GHz and producing its harmonics of which the fourth, eighth, 16th, 24th, and 32nd were available. A superconducting magnet (Oxford Instruments) capable of reaching a field of 17 T was employed.

Magnetic susceptibility data of powdered samples were measured with a SQUID magnetometer (Quantum Design MPMSXL-5) over the temperature range 1.8−300 K at the magnetic induction of 0.5 T. Corrections for the sample holders were applied. Diamagnetic corrections for the molecules were determined from Pascal's constants.[10]

Single-Crystal Structure Determination. The single-crystal diffraction data for **2a**, **3**, and **4** were collected at room temperature on an Oxford Diffraction KM4 CCD diffractometer employing Mo Kα radiation with $\lambda = 0.71073$ Å. The reflections were measured with ω-2θ method and numerical absorption corrections were applied.[11] All figures have been prepared in ORTEP and DIAMOND v. 2.1e programs.[12]

Synthesis. A blue solution of $Cu(CF_3COO)_2$, prepared by reacting CF_3COOH with CuO, was evaporated to dryness, and the resulting green solid was used in subsequent preparations.

$[Cu(CF_3COO)_2\cdot(CH_3CN)]_2$ (1). Copper trifluoroacetate was dissolved in CH_3CN to form a saturated solution at ca. 60 °C in a closed vial. Slow temperature lowering resulted in formation within hours of very large (up to 10 mm × 3 mm × 2 mm) green, transparent crystals. The substance is very hygroscopic and flows when exposed to humid air. The identity of the product, which was described previously,[5] was confirmed by the X-ray determination of its crystal lattice parameters.

$[Cu(CF_3COO)_2\cdot(quin)]_2$ (2). The method described in ref 6 was followed. Violet powder $Cu(CF_3COO)_2(quin)_2$, obtained by reacting copper trifluoroacetate with quinoline in ethanolic solution, was heated to ca. 80 °C in a Petri dish until it turned green. The crude green product was dissolved in 99.8% benzene or in toluene and filtered. The commercial solvents were not dried, which may have aided in obtaining some of the compounds described below. Evaporation of a solution at elevated temperature, close to the solvent boiling point and under protection from humidity, resulted in formation of large yellow-green X-ray quality crystals of **2**. IR bands: 3422, 3094, 2955, 2853, 1704, 1599, 1565, 1512, 1441, 1404, 1379, 1315, 1198, 1146, 1056, 958, 846, 808, 795, 780, 728, 613, 522, 497, 475 cm^{-1}. The product identity was confirmed by X-ray determination of its lattice constants.[6]

$[Cu_4(OH)_2(CF_3COO)_8(quin)_2]^{2-}(quinH^+)_2$ (2a). Compound **2** turns blue on prolonged exposure to humid air. This blue solid product that will be called **2a** here was described previously,[6] and the formula $Cu(CF_3COO)_2(C_9H_7N)(H_2O)$ was proposed on the basis of chemical analysis only. In our case, the yellow-green crystals of **2** converted to blue on humid air, seemingly without crystal destruction. However, the product turned out not to consist of single crystals. Blue crystalline product of X-ray quality was obtained by exposing solution of dimer **2** in benzene to humid air and an unprecedented tetranuclear structure was revealed by X-ray diffractometry (see below). IR spectra confirmed that the two blue products are the same compound. Warming the blue powder **2a** to ~80 °C converts it back to the yellow-green **2**. Apparently, **2** and **2a** convert to each other in the process

$$2[Cu(CF_3COO)_2(quin)]_2 + 2H_2O \leftrightarrow [Cu_4(OH)_2(CF_3COO)_8(quin)_2]^{2-}(quinH^+)_2$$

The Moreland's formula[6] $Cu(CF_3COO)_2(C_9H_7N)(H_2O)$ contains two more water molecules per tetrameric unit than ours for **2a** (molar mass 1711.0) and the two formulas are difficult to distinguish by chemical analysis.

Analysis of 2a. Cu 14.8, C 36.7, H 2.69, N 3.45; calcd for $Cu_4C_{52}F_{24}H_{32}N_4O_{18}$ Cu 14.86, C 36.50, H 1.88 N 3.27.

$Cu_4O(CF_3COO)_6(quin)_4\cdot(C_6H_5CH_3)_{0.6}$ (3) and $Cu_4O(CF_3COO)_6(quin)_4\cdot(C_6H_6)_{0.8}$ (4). These substances can be obtained from the crude green powder (above) or from the blue product **2a**. Approximately 1 g of the substrate was dissolved by boiling in 30 mL of benzene or toluene, respectively. The solution was left to cool slowly in a tightly closed flask causing precipitation of small green crystals of **3** or **4** within hours. Obtaining X-ray quality crystals was difficult. IR bands for **3** (cm^{-1}): 3422, 3093, 2948, 2853,1686, 1599, 1559, 1513, 1442, 1406, 1378, 1316, 1199, 1146, 1058, 960, 846, 810, 795, 781, 727, 638, 613, 522, 497, 468. IR bands for **4** (cm^{-1}): 3422, 3085, 2954, 2859,1686, 1599, 1561, 1513, 1443, 1406, 1379, 1316, 1199, 1146, 1058, 960, 845, 810, 795, 782, 727, 638, 613, 522, 497, 468.

Analysis of 3 $[Cu_4O(CF_3COO)_6(quin)_4]\cdot 0.6C_6H_5CH_3$. Cu 16.7, C 41.0, H 2.7, N 3.8; calcd for $Cu_4C_{52.2}H_{32.8}N_4F_{18}O_{13}$ (MW = 1520.2) Cu 16.72, C 41.24, H 2.17, N 3.68.

Analysis for 4. Cu 16.7, C 40.4, H 2.8, N 3.98; calcd for $Cu_4C_{52.8}H_{32.8}N_4F_{18}O_{13}$ (MW = 1527.4) Cu 16.64, C 41.52, H 2.16, N 3.67:

Some samples of **3** and **4** were found by EPR to be contaminated by **2**, but very pure crystalline samples of all three substances were also prepared. Both **3** and **4** convert on humid air to a blue solid product **3a**, which is different from **2a**. Heating **3a** does not convert it back to **3** nor to **2**, but **3** or **4** can be obtained by boiling **3a** in toluene or benzene, respectively. Analytical data for **3a**: Cu 16.1, C 38.8, H 2.9, N 3.9.

CCDC 733624, 733605, and 733606 contain the supplementary crystallographic data for **2a**, **3**, and **4**, respectively. These data can be obtained free of charge from the Cambridge Crystallographic Data Centre via www.ccdc.cam.ac.uk/data_request/cif.

Note on the Analysis. Fluorine-containing compounds pose difficulties when using standard instrumentation for the C, H, N analysis,[13] which in our case were augmented by copper trifluoroacetate volatility and are reflected in our poor results for H. Problems were also encountered in AAS analysis and for that reason copper was also determined iodometrically.[13]

Results and Discussion

IR Spectra. Asymmetric and symmetric stretching vibrations of the carboxylic group were detected at: $\nu_{as}(COO) = 1686$ cm^{-1} for **3** and **4** and at 1704 cm^{-1} for **2**, while $\nu_s(COO)$ appeared at

(9) Hassan, A. K.; Pardi, L. A.; Krzystek, J.; Sienkiewicz, A.; Goy, P.; Rohrer, M.; Brunel, L.-C. *J. Magn. Reson.* **2000**, *142*, 300–312.
(10) O'Connor, C. J. *Prog. Inorg. Chem.* **1982**, *29*, 203–283.
(11) *CrysAlis RED* and *CrysAlis CCD*; Oxford Diffraction: Abingdon, Oxfordshire, England, 2000.
(12) Brandenburg, K. *DIAMOND, Release 2.1e*; Crystal Impact GbR: Bonn, Germany, 2001. Farrugia, L. J. *J. Appl. Crystallogr.* **1997**, *30*, 565.
(13) Campbell, A. D.; MacDonald, A. M. G. *Anal. Chim. Acta* **1962**, *26*, 275–280. Hall, W. T., Williams, R. S. In *The Chemical and Metallographic Examination of Iron, Steel and Brass*; McGraw-Hill: New York, 1921.

1441−1443 cm^{-1}. The difference $\Delta\nu = \nu_{as}(COO) - \nu_{s}(COO)$ for **3** and **4** is 244 cm^{-1} but is 263 cm^{-1} for **2**. These values are in accord with the bridging carboxylate coordination in **2**, **3**, and **4**.[14] The ν_{ring} and δ_{ring} band shifts, typical for coordinated quinoline, were observed over the range 600−1600 cm^{-1}.[15] In the spectra of **3** and **4** a sharp absorption band at 638 cm^{-1} was detected. This band is missing from the spectra of the free quinoline, trifluoroacetates, and also of complex **2**. Therefore it was assigned to the vibration of the Cu_4O core. In the case of compounds $[Cu_4(\mu_4\text{-}O)(bahped)_2](ClO_4)_2$[16] and $[Cu_4Cl_6(\mu_4\text{-}O)(OSR_2)_4]$ (R = Et, ^nBu),[17] the Cu_4O bands were observed at 566−583 cm^{-1}, whereas they appeared at 581−592 cm^{-1} in copper 2,6-bis(morpholinomethyl)-4-methylphenol complexes.[18]

Blue Products 2a and 3a Compared to Green Complexes 2−4. Although the carboxylate $\Delta\nu$ of 254 cm^{-1} in **3a** is altered compared to tetramers **3** and **4**, it is still within the bridging carboxylate range. The μ_4-O bridge seems to be retained in **3a**.[19] There is some IR evidence that in **3** and **4** quinoline has been oxidized on exposure to humid air to form quinoline *N*-oxide that interacts with copper via the oxygen atom from the highly polarized N→O group. The oxidation may not have occurred for all quinoline molecules, because the new bands ν(C═N) = 1590, ν(N−O) = 1272, ν(N−O) = 1244 add to the old ones rather than replacing them, and no effect on EPR parameters of replacing N by O was observed for the blue product **3a** (see below). The intensity increase of the bands at 1145 and 1163 cm^{-1} may be attributed to the appearance of the δ(N−O) vibration. The off-plane C−H bands are seen at 810 and 727 cm^{-1}. The changes in IR described here are accompanied by drastic changes in the magnetic properties and EPR spectra.

Blue species **2a** exhibits no μ_4-O band. $\Delta\nu$ of 250 cm^{-1} is within the range of bridging carboxylate. The 1404 cm^{-1} band splits into two bands at 1400 and 1412 cm^{-1}, and the 785 cm^{-1} band intensity is reduced compared to that of **3a**.

X-ray Structure of $[Cu_4O(CF_3COO)_6(quin)_4]\cdot 0.6C_6H_5CH_3$ (3, Figure 1). The details of data collection are given in Table 1. The crystal dimensions were 0.10 mm × 0.06 mm × 0.62 mm. The structure was solved by direct methods and refined with a full-matrix least-squares procedure on F^2 using the SHELX-97 program package.[20] Because of the high dynamics exhibited by the CF_3 groups and one of the quinoline molecules, geometrical and/or thermal restraints were applied for these parts of the structure. Similarly, such restraints were applied for the partially occupied toluene sites. Hydrogen atoms were added according to geometry and not refined. They were omitted for toluene molecule as it exhibits disorder and high temperature factors leading to a low-quality electron density maps in this region. This data set is of the lowest quality of the three reported here. As a consequence, the goodness-of-fit and *R* parameters are slightly higher than in **4** and **2a**.

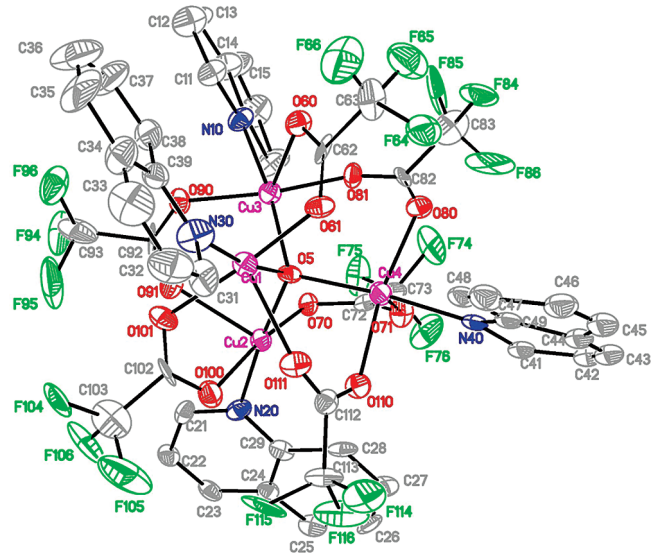

Figure 1. Molecular structure of **3**. The copper, oxygen, nitrogen, carbon, and fluorine atoms are drawn in magenta, red, blue, gray, and green, respectively. Hydrogen atoms are omitted and only one of the disordered positions of quinoline and of each disordered fluorine atom is shown. Thermal ellipsoids are drawn at 20% for the image clarity. The molecular structure of **4** is shown in Figure S7 in Supporting Information.

Structure Description. Important bond lengths and angles for **3** and **4** are given in Table 2. $[Cu_4O(CF_3COO)_6(quin)_4]\cdot 0.6C_6H_5CH_3$ (**3**) crystallizes in the orthorhombic *Pbca* space group. The asymmetric unit contains 1 tetranuclear molecule and 0.6 molecules of toluene.

The O^{2-} anion O5 at the molecule center is surrounded by four copper(II) ions forming a distorted tetrahedron with the Cu−Cu distances varying from 3.069 to 3.376 Å. The coordination sphere of each copper atom adopts a distorted square pyramid geometry owing to the Jahn−Teller effect. The copper coordination sphere consists of three oxygen atoms of carboxylate anions, one central O^{2-} anion, and one nitrogen atom of the quinoline molecule. The nitrogen atom in the base of each square pyramid is bound in trans position versus the central O^{2-} anion. Similarly, two carboxylate oxygen atoms are in trans position versus each other. The coordination spheres are completed by the third carboxylate oxygen atom coordinated in the axial position, at distances of 2.257(12)−2.372(11) Å, which are longer by 0.3−0.4 Å than those of the carboxylate oxygen atoms found in the basal plane. The Cu−O(carboxylate) bond lengths in the basal plane (1.929(12)−1.992(11) Å) are similar to the Cu−O5 bond lengths (1.949(8) and 1.969(9) Å). Nitrogen is bound at a slightly longer distance (2.009(17)−2.035(14) Å).

All carboxylates are involved in bridging interactions. However, there are two types of carboxylate bridges. In the first one a carboxylate joins an axial position of one copper atom with an equatorial position of another copper atom. The other type of bridge is symmetric and joins equatorial positions of two copper atoms. There are four bridges of the former and two of the latter type in the tetranuclear molecule. The longest intermetallic distances are found for the Cu atoms that are joined by the symmetric carboxylate groups. These intermetallic distances as well as the torsion angles M−O−C−O/O−C−O−M (−9.93°/34.87°) indicate that copper atoms are bound in a syn/syn arrangement (ideal values 0°/0°). The distances C−O(carboxylate) range from 1.20(2) to 1.25(2) Å, and this bond length depends neither on the carboxylate coordination mode nor on

(14) Nakamoto, K. In *Infrared and Raman Spectra of Inorganic and Coordination Compounds, part B*; John Wiley & Sons: New York, 1997; pp 59−62; 276−282.
(15) Ozel, A. E.; Buyukmurat, Y.; Akyuz, S. *J. Mol. Struct.* **2001**, *565−566*, 455–462.
(16) Bera, M.; Wong, W. T.; Aromi, G.; Ribas, J.; Ray, D. *Inorg. Chem.* **2004**, *43*, 4787–4789.
(17) Guy, J. T., Jr.; Cooper, J. C.; Gilardi, R. D.; Flippen-Anderson, J. L.; George, C. F., Jr. *Inorg. Chem.* **1988**, *27*, 635–638.
(18) Teipel, S.; Griesar, K.; Haase, W.; Krebs, B. *Inorg. Chem.* **1994**, *33*, 456–464.
(19) Kalyanasundaram, R.; Navaneetham, N. S.; Soundararajan, S. *Proc. Indian Acad. Sci.* **1985**, *95*, 235–242.
(20) Sheldrick, G. M. *Acta Crystallogr.* **2008**, *A64*, 112–122. Sheldrick, G. M. *SHELXS97*, *SHELXL97*, and *CIFTAB*; University of Göttingen: Germany, 1997.

Table 1. Details of Crystallographic Data Collection and Structure Refinement for **3** and **4**

compound	toluene solvate (**3**)	benzene solvate (**4**)
formula	$C_{52.2}H_{32.8}Cu_4F_{18}N_4O_{13}$	$C_{52.8}H_{32.8}Cu_4F_{18}N_4O_{13}$
formula weight	1520.2	1527.4
crystal system	orthorhombic	monoclinic
space group	*Pbca* (No. 61)	*P*2/*c* (No. 13)
	unit cell dimensions	
a [Å]	15.278(3)	21.933(4)
b [Å]	23.227(5)	11.176(2)
c [Å]	34.895(7)	23.927(5)
β [deg]	90	97.41(3)
V [Å^3]	12383(4)	5816(2)
Z	8	4
D_{calc} [Mg/m^3] [g/cm^3]	1.630	1.709
absorption coefficient [mm^{-1}]	1.471	1.564
F(000)	5808	2971
crystal size [mm]	0.10 × 0.06 × 0.62	0.51 × 0.22 × 0.08
θ range for data collection [deg]	2.11−18.85	2.37−20.81
index ranges	$-13 < h < 13$	$-21 < h < 21$
	$-21 < k < 18$	$-8 < k < 11$
	$-31 < l < 31$	$-23 < l < 23$
reflections collected/independent reflections	41075/4861 [R(int) = 0.1223]	23482/6077 [R(int) = 0.0704]
transmission maximum/minimum	0.9308/0.6107	0.8904/0.4996
refinement method	full-matrix least-squares on F^2	
goodness-of-fit on F^2	1.266	1.075
final *R* indices [$I > 2\sigma(I)$][a]	R1 = 0.1049, wR2 = 0.2294	R1 = 0.0828, wR2 = 0.1981
R indices (all data)[a]	R1 = 0.1098, wR2 = 0.2330	R1 = 0.1071, wR2 = 0.2195
largest diff peak and hole [e A^{-3}]	0.485/−0.333	0.683/−0.905

[a] $R1 = \Sigma||F_o| - |F_c||/\Sigma|F_o|$. $wR2 = [\Sigma w(F_o^2 - F_c^2)^2/\Sigma(w|F_o|^2)^2]^{1/2}$.

its contacts to copper. Disorder of one quinoline molecule and of all but one CF_3 groups is observed. Assumption of the alternative orientations for quinoline and the CF_3 groups led to a significant model improvement. There are numerous H-bonds between the quinoline H atoms and fluorine atoms of CF_3, which stabilize both the disordered orientations of CF_3 groups and of the quinoline molecule. In the latter case both orientations are related approximately by a rotation about the N40−Cu4−N50 angle bisector. The distance Cu−N for the alternative disordered nitrogen atom is the longest one, while the axial bond elongation is the shortest. This additional position of nitrogen atom leads to a very unfavorable geometry of the coordination polyhedron, as the bond angles formed by this copper atom are far from 90° or 180° expected for a square pyramid. The ordered aromatic quinoline rings are planar with rmsd 0.02−0.04 Å, whereas the rmsds for the disordered one are 0.069 and 0.097 Å.

Cu1, Cu2, and Cu3 atoms are removed by approximately 0.05 Å (0.056−0.057 Å) from their basal planes toward the axial oxygen atom. The disordered quinoline molecule adopting two discrete positions defines two distinct basal planes that differ only by one nitrogen atom (N40 or N50). The Cu4 atom leans out by −0.016 and 0.191 Å from the basal planes involving N40 and N50 atoms, respectively. In the first case Cu moves in the direction opposite to the axial O71 oxygen atom, contrary to the shifts observed for Cu1, Cu2, and Cu3 atoms. In the second case the Cu4 atom shifts out of the N50 basal plane by 0.191 Å toward O71, as was observed for other Cu atoms. However, this basal plane is significantly distorted as it shows rmsd equal to 0.269 Å, whereas in other cases it does not exceed 0.08 Å. The crystal packing and the hydrogen bond system is described in Supporting Information.

X-ray Structure of $[Cu_4O(CF_3COO)_6(quin)_4]\cdot 0.8C_6H_6$ (4). Similarly as it was done for the toluene solvate, the geometrical and/or thermal restraints were applied to the CF_3 groups and one of the quinoline molecules as well as to the partially occupied benzene sites. Hydrogen atoms were added according to geometry and not refined. They were omitted for the benzene molecule as it exhibits partial occupancy and high temperature factors leading to low quality of electron density maps in this region.

Structure Description. The $[Cu_4O(CF_3COO)_6(quin)_4]\cdot 0.8C_6H_6$ complex crystallizes in the monoclinic centrosymmetric *P*2/*c* space group. The asymmetric unit contains one tetranuclear molecule and a benzene molecule that was refined with 0.8 occupancy and positioned around a 2-fold axis. Two atoms of benzene molecule (C121 and C123) are positioned strictly on the 2-fold axis in special positions. C122 and C124 atoms and their images generated by the 2-fold axis ($-x$, y, $-z + 1/2$) complete the benzene molecule. The molecular structure is essentially the same as that of the toluene solvate. The Cu−O(carboxylate) bond lengths in the basal plane (1.949(9)−1.992(7) Å) are similar to the Cu−O5 bond lengths in **3** (1.949(7)−1.966(6) Å). The nitrogen atom of the ordered quinoline molecules is bound at a slightly longer distance (2.022(11)−2.034(12) Å). The axial oxygen atoms were found at distances 2.297(7)−2.389-(11) Å.

The most significant differences between structures of **3** and **4** concern the geometry around the Cu4 atom, which is coordinated by the disordered quinoline molecules. In **4** we observe additional electron density picks lying out of the N40 ring plane, whereas in **3** both orientations are related by a bisector of the N40−Cu4−N50 angle. This time, the alternative orientation (N50) reveals rocking by approximately 1 Å and tilting by 35.9° versus the N40 ring, and it is stabilized by a very short intramolecular H-bond to F85. The Cu−N bond lengths found for the disordered quinoline molecule present two extreme values: Cu−N40 is the longest (2.13 Å), whereas this distance in the alternative orientation is in the usual range found in this structure (2.01 Å) and falls within the typical range of the Cu−O bond lengths.

The orientation of the copper basal planes is similar in both tetramers. Every basal plane is almost perpendicular to two others and tilted by 25.5° (Cu2/Cu3) or 28.5° (Cu1/Cu4) to the third plane. This effect is observed for basal planes with copper

Table 2. Selected Interatomic Distances [Å] and Angles [deg] for **3** and **4**

3				**4**			
distance [Å]		angle [deg]		distance [Å]		angle [deg]	
Cu(1)−O(61)	1.967(11)	O(61)−Cu(1)−O(5)	90.7(4)	Cu(1)−O(5)	1.966(6)	O(5)−Cu(1)−O(70)	88.7(3)
Cu(1)−O(5)	1.969(9)	O(61)−Cu(1)−O(101)	168.7(4)	Cu(1)−O(70)	1.968(8)	O(5)−Cu(1)−O(60)	100.4(3)
Cu(1)−O(101)	1.985(12)	O(5)−Cu(1)−O(101)	100.6(4)	Cu(1)−O(60)	1.992(7)	O(70)−Cu(1)−O(60)	170.6(3)
Cu(1)−N(30)	2.009(17)	O(61)−Cu(1)−N(30)	84.6(6)	Cu(1)−N(10)	2.024(8)	O(5)−Cu(1)−N(10)	161.9(3)
Cu(1)−O(111)	2.339(11)	O(5)−Cu(1)−N(30)	169.9(7)	Cu(1)−O(81)	2.297(7)	O(70)−Cu(1)−N(10)	88.5(3)
Cu(2)−O(5)	1.949(8)	O(101)−Cu(1)−N(30)	84.3(6)	Cu(2)−O(101)	1.949(9)	O(60)−Cu(1)−N(10)	83.5(3)
Cu(2)−O(100)	1.988(13)	O(61)−Cu(1)−O(111)	92.3(5)	Cu(2)−O(5)	1.956(6)	O(5)−Cu(1)−O(81)	95.3(3)
Cu(2)−O(70)	1.992(11)	O(5)−Cu(1)−O(111)	92.1(4)	Cu(2)−O(90)	1.984(8)	O(70)−Cu(1)−O(81)	92.9(3)
Cu(2)−N(20)	2.035(14)	O(101)−Cu(1)−O(111)	87.4(5)	Cu(2)−N(20)	2.034(11)	O(60)−Cu(1)−O(81)	84.1(3)
Cu(2)−O(91)	2.337(13)	N(30)−Cu(1)−O(111)	96.9(7)	Cu(2)−O(71)	2.389(11)	N(10)−Cu(1)−O(81)	102.7(3)
Cu(3)−O(81)	1.929(12)	O(5)−Cu(2)−O(100)	97.9(5)	Cu(3)−O(5)	1.949(7)	O(101)−Cu(2)−O(5)	99.0(3)
Cu(3)−O(90)	1.945(12)	O(5)−Cu(2)−O(70)	93.0(4)	Cu(3)−O(80)	1.982(8)	O(101)−Cu(2)−O(90)	169.4(3)
Cu(3)−O(5)	1.968(9)	O(100)−Cu(2)−O(70)	168.4(5)	Cu(3)−O(100)	1.980(9)	O(5)−Cu(2)−O(90)	91.7(3)
Cu(3)−N(10)	2.014(15)	O(5)−Cu(2)−N(20)	175.0(6)	Cu(3)−N(30)	2.022(11)	O(101)−Cu(2)−N(20)	86.2(4)
Cu(3)−O(60)	2.372(11)	O(100)−Cu(2)−N(20)	81.6(5)	Cu(3)−O(110)	2.314(11)	O(5)−Cu(2)−N(20)	171.7(5)
Cu(4)−O(5)	1.960(9)	O(70)−Cu(2)−N(20)	87.1(5)	Cu(4)−N(50)	2.01(5)	O(90)−Cu(2)−N(20)	83.2(4)
Cu(4)−O(110)	1.970(11)	O(5)−Cu(2)−O(91)	92.8(4)	Cu(4)−O(5)	1.966(7)	O(101)−Cu(2)−O(71)	88.1(5)
Cu(4)−O(80)	1.972(12)	O(100)−Cu(2)−O(91)	90.8(5)	Cu(4)−O(61)	1.986(9)	O(5)−Cu(2)−O(71)	93.5(3)
Cu(4)−N(40)	2.03(3)	O(70)−Cu(2)−O(91)	92.4(5)	Cu(4)−O(111)	1.974(12)	O(90)−Cu(2)−O(71)	91.4(4)
Cu(4)−N(50)	2.15(3)	N(20)−Cu(2)−O(91)	92.1(6)	Cu(4)−N(40)	2.13(3)	N(20)−Cu(2)−O(71)	93.3(6)
Cu(4)−O(71)	2.257(12)	O(81)−Cu(3)−O(90)	170.9(5)	Cu(4)−O(91)	2.349(12)	O(5)−Cu(3)−O(80)	92.3(3)
Cu(1)−Cu(2)	3.3702(27)	O(81)−Cu(3)−O(5)	97.9(4)	Cu(1)−Cu(2)	3.0199(19)	O(5)−Cu(3)−O(100)	98.0(3)
Cu(1)−Cu(3)	3.0694(28)	O(90)−Cu(3)−O(5)	90.7(4)	Cu(1)−Cu(3)	3.0882(18)	O(80)−Cu(3)−O(100)	169.7(4)
Cu(1)−Cu(4)	3.1007(29)	O(81)−Cu(3)−N(10)	87.4(6)	Cu(1)−Cu(4)	3.3817(21)	O(5)−Cu(3)−N(30)	175.90(4)
Cu(2)−Cu(3)	3.1413(27)	O(90)−Cu(3)−N(10)	83.7(6)	Cu(2)−Cu(3)	3.3960(20)	O(80)−Cu(3)−N(30)	87.3(4)
Cu(2)−Cu(4)	3.1426(27)	O(5)−Cu(3)−N(10)	172.1(5)	Cu(2)−Cu(4)	3.1047(23)	O(100)−Cu(3)−N(30)	82.3(4)
Cu(3)−Cu(4)	3.3764(27)	O(81)−Cu(3)−O(60)	85.6(4)	Cu(3)−Cu(4)	3.1789(28)	O(5)−Cu(3)−O(110)	91.9(3)
		O(90)−Cu(3)−O(60)	96.7(5)			O(80)−Cu(3)−O(110)	90.1(4)
		O(5)−Cu(3)−O(60)	95.0(4)			O(100)−Cu(3)−O(110)	90.6(4)
		N(10)−Cu(3)−O(60)	91.2(6)			N(30)−Cu(3)−O(110)	92.2(5)
		O(5)−Cu(4)−O(110)	90.2(4)			N(50)−Cu(4)−O(5)	156.1(11)
		O(5)−Cu(4)−O(80)	100.2(4)			N(50)−Cu(4)−O(61)	93.3(10)
		O(110)−Cu(4)−O(80)	169.5(5)			O(5)−Cu(4)−O(61)	97.4(3)
		O(5)−Cu(4)−N(40)	174.5(8)			N(50)−Cu(4)−O(111)	75.2(11)
		O(110)−Cu(4)−N(40)	85.1(8)			O(5)−Cu(4)−O(111)	92.9(5)
		O(80)−Cu(4)−N(40)	84.4(8)			O(61)−Cu(4)−O(111)	168.5(5)
		O(5)−Cu(4)−N(50)	150.5(8)			N(50)−Cu(4)−N(40)	29.9(10)
		O(110)−Cu(4)−N(50)	88.2(8)			O(5)−Cu(4)−N(40)	173.7(8)
		O(80)−Cu(4)−N(50)	82.6(8)			O(61)−Cu(4)−N(40)	78.0(8)
		N(40)−Cu(4)−N(50)	32.4(10)			O(111)−Cu(4)−N(40)	92.1(9)
		O(5)−Cu(4)−O(71)	92.9(4)			N(50)−Cu(4)−O(91)	109.1(14)
		O(110)−Cu(4)−O(71)	93.1(5)			O(5)−Cu(4)−O(91)	92.0(3)
		O(80)−Cu(4)−O(71)	86.7(5)			O(61)−Cu(4)−O(91)	91.8(4)
		N(40)−Cu(4)−O(71)	84.5(10)			O(111)−Cu(4)−O(91)	93.0(5)
		N(50)−Cu(4)−O(71)	116.6(8)			N(40)−Cu(4)−O(91)	83.9(8)
		Cu(2)−O(5)−Cu(4)	107.0(4)			Cu(3)−O(5)−Cu(4)	108.6(3)
		Cu(2)−O(5)−Cu(3)	106.6(4)			Cu(3)−O(5)−Cu(2)	120.8(3)
		Cu(4)−O(5)−Cu(3)	118.5(5)			Cu(4)−O(5)−Cu(2)	104.7(3)
		Cu(2)−O(5)−Cu(1)	118.7(5)			Cu(3)−O(5)−Cu(1)	104.1(3)
		Cu(4)−O(5)−Cu(1)	104.2(4)			Cu(4)−O(5)−Cu(1)	118.7(3)
		Cu(3)−O(5)−Cu(1)	102.5(4)			Cu(2)−O(5)−Cu(1)	100.7(3)

atoms joined by carboxylate anion coordinated in equatorial positions to both centers. In **4** all Cu atoms are shifted by 0.009−0.167 Å from the basal plane toward the axial oxygen atom. Contrary to **3**, such shift is observed also for Cu4 atom that is bound to disordered quinoline molecule, and it adopts the smallest (N40) and the biggest values (N50). The angles around Cu4 atom reveal that its coordination sphere in **4** is less distorted than in **3**. This conclusion is also confirmed by smaller rmsd (0.031−0.173 Å) of atoms from the basal plane than observed for **3**. Surprisingly, it reaches the largest magnitude for the basal plane involving the N10 atom and coordination sphere around Cu1, whereas for the disordered quinoline it is smaller: 0.076 and 0.160 Å for the N40 and N50 basal planes, respectively.

All carboxylates are involved in bridging interactions in the same manner as observed in **3**. The distances C−O(carboxylate) range from 1.207(17) to 1.264(24) Å, and these bond lengths exhibit no correlation with the coordination mode and contacts to copper.

The distances between the metal centers forming a tetrahedron around the central O5 atom vary from 3.020(2) to 3.396(2) Å. The intermetallic distances as well as the torsion angles M−O−C−O/O−C−O−M (6.27−46.59°) indicate that those copper atoms are bound in a syn/syn arrangement. However, the torsion angles as well as the intermetallic distances are somewhat larger than found for **3**.

Important hydrogen bonds are listed and the crystal packing is described in Supporting Information.

Comparison of 3 and 4 to Selected Known Trifluoroacetato-Bridged Copper Dimers and Tetramers. In dimer **2**, the quinoline nitrogen is in an axial position of Cu, whereas it is an equatorial ligand in the tetramers **3** and **4**. There are no other

significant differences between **3**, **4**, and **2** as far as the bond lengths in the copper coordination sphere are concerned. In the dimer, all oxygen atoms are found in the basal plane and their contacts to copper (1.956(7)−1.990(6) Å)[6] are similar to those in the square pyramid base in the tetramers. The Cu−N bond to the axial quinoline is slightly longer (2.109(6) Å) than equatorial bonds, which results from the Jahn−Teller effect. The most significant geometric difference is the metal−metal distance, which equals 2.886(4) Å in **2** and is one of the longest separations found in copper paddlewheel dimers. However, it is still shorter by 0.2−0.5 Å than in our tetramer structures. The Cu-basal plane distance (0.321 Å) is also much larger in the dimer than that found in the tetramers. The average O−C−O and Cu−O−C angles in **2**, of 129.3(9)° and 124.7(6)°, respectively, fall within the range observed in **3** and **4** (Table 2).

A tetramer with formula $[Cu_2(OH)(CF_3COO)_3(quin)_2]_2$ is known that differs from our formulas by two hydroxyl groups replacing a single O^{2-} anion.[21] However, it is completely different structurally from our compounds. The four copper atoms in it are not chemically identical. There are two inner metal sites (Cu1 and Cu1′) and two outer ones (Cu2 and Cu2′), differing in composition of the coordination sphere. The inner atom polyhedra share a basal edge, whereas the outer atoms share only one basal corner with the inner copper atoms. That corner is occupied by an OH group, which creates a H-bond to a free oxygen atom of the trifluoroacetate ligand that is monodentately coordinated to Cu2. No monodentate carboxylates are present in **3** and **4**.

Single-Crystal Structure Determination of $\{[Cu_2(OH)(CF_3COO)_4(quin)]^-(quinH^+)\}_2$ (2a, Figure 2). The instrumental details are described in the Experimental Section. Crystal data and structure refinement details are given in Table 3. The crystal dimensions were 0.240 mm × 0.084 mm × 0.126 mm. The structure of **2a** was solved by direct methods and refined with a full-matrix least-squares procedure on F^2 using the SHELX-97 program package.[20] Contrary to tetramers **3** and **4**, this structure does not exhibit any significant disorder. Alternative positions were allowed for one CF_3 group only, which led to a reasonable temperature displacement and an overall model improvement. Hydrogen atoms were added according to geometry and refined as riding atoms with fixed temperature displacement. H atoms of the functional groups (H5 and H60) were treated exceptionally; their positions as well as the temperature displacement parameters were refined without any restraints. They are stable, indicating that the uncoordinated quinoline molecule and oxygen O5 are protonated.

It is noteworthy that our summary formula and that proposed by Moreland,[6] $Cu(CF_3COO)_2(quin)(H_2O)$ (which was assumed to be monomeric), differ only by $2H_2O$ per a tetranuclear unit.

Structure Description. Selected bond lengths and angles are listed in Table 4. The $\{[Cu_2(OH)(CF_3COO)_4(quin)]^-(quinH^+)\}_2$ complex crystallizes in the triclinic *P*-1 space group. The asymmetric unit contains two counterions: one-half of the tetramer is an anion and one protonated quinoline molecule is a cation. The second half of the tetramer is generated by the $(1 - x,-y,1 - z)$ symmetry operator. The coordination sphere of both crystalographically independent copper atoms (inner Cu1 and outer Cu2) adopts distorted square pyramid geometry owing to the Jahn−Teller effect, with a significant elongation of the apical bond by 0.20−0.25 Å. The coordination spheres of both copper atoms differ significantly. Cu1 is bound only to two hydroxyl oxygen atoms and to three carboxylate anions, whereas in the Cu2 coordination sphere one OH^- group is substituted by a quinoline molecule. In both cases the apical position is occupied by a carboxylate oxygen atom. In the base of Cu1, both OH^- groups are mutually in cis positions. Accordingly, the two carboxylates are also bound in cis positions. Contrary to this, the quinoline molecule and hydroxyl group are in trans positions around Cu2 atom and the two carboxylates are also in trans positions. However, in both cases in the basal plane there is one bridging and one monodentately bound anion, whereas the apical position is occupied by another bridging trifluoroacetate anion. Consequently, the bridging carboxylates coordinate to an axial position of one copper atom and an equatorial of another. The basal planes of Cu1 and Cu1#1 are related by inversion center, while the Cu2 basal plane is almost perpendicular to them (89.27(9)°). In the basal planes of both copper coordination polyhedra, the carboxylate oxygen atoms exhibit the shortest Cu−O separation whereas the hydroxyl group and quinoline nitrogen atom are bound at a slightly longer (by 0.03 Å) distance. All four copper atoms lie exactly in one plane and form a slightly distorted diamond whose short axis joins Cu1 and Cu1#1 (3.005 Å) while the long one joins Cu2 and Cu2#1 (6.022 Å). The diamond edges are approximately 3.36 Å long. The O5 atoms of OH^- anions act as μ_3 bridges

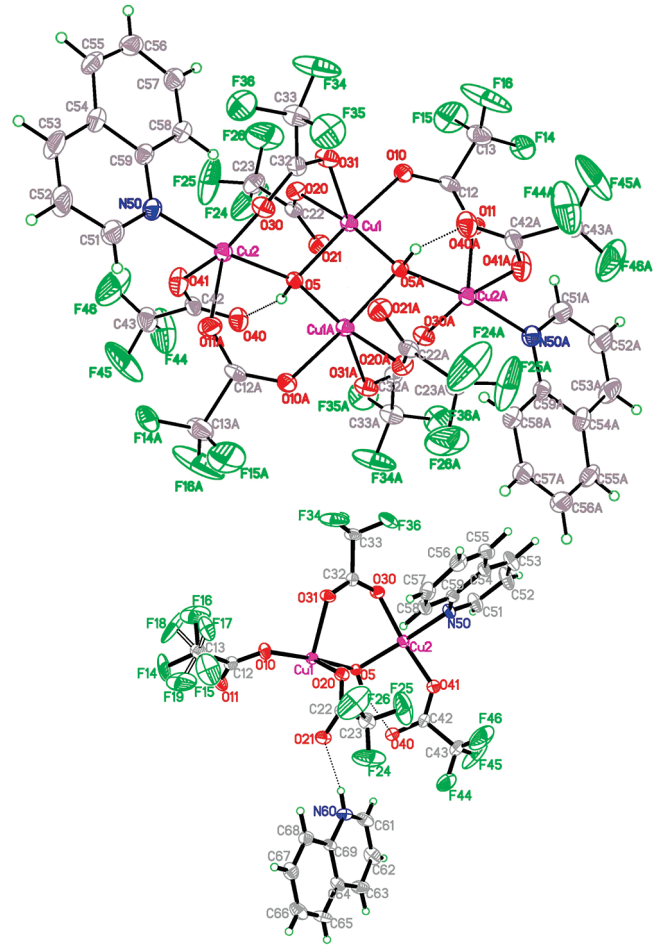

Figure 2. (Top) Structure of the tetranuclear anion $[Cu_2OH(CF_3COO)_4(quin)]_2^{2-}$ in **2a**. (Bottom) One-half of the tetranuclear anion and the noncoordinated $quinH^+$ cation forming hydrogen bonds N60−H60···O21 (1.95 Å) and N60−H60···F24 (2.82 Å) to the anion.

(21) Little, R. G.; Moreland, J. A.; Yawney, D. B. W.; Doedens, R. J. *J. Am. Chem. Soc.* **1974**, *96*, 3834–3842.

Table 3. Crystal Data and Structure Refinement for $\{[Cu_2(OH)(CF_3COO)_4(quin)](quinH)\}_2$ (**2a**)

formula	$C_{26}H_{16}Cu_2F_{12}N_2O_9$
formula weight	855.49
temperature [K]	293(2)
wavelength [Å]	0.71073
crystal system	triclinic
space group	*P*-1 (No. 2)
unit cell dimensions [Å] and [deg]	
a [Å]	10.480(2)
b [Å]	13.107(3)
c [Å]	13.399(3)
α (deg)	114.54(3)
β (deg)	92.11(3)
γ (deg)	102.31(3)
volume [Å^3]	1619.4(6)
Z	2
D_{calc} [Mg/m^3] [g/cm^3]	1.754
absorption coefficient [mm^{-1}]	1.435
F(000)	848
crystal size [mm]	0.240 × 0.084 × 0.126
θ range for data collection [deg]	2.43 to 23.26
limiting indices/index ranges	$-8 \le h \le 11$, $-14 \le k \le 14$, $-14 \le l \le 14$
reflections collected/reflections unique	9318/4652 [$R_{int} = 0.0350$]
transmission maximum/minimum	0.78650/0.92785
completeness to $\theta = 23.26$ [%]	99.7
refinement method	full-matrix least-squares on F^2
data/restraints/parameters	4652/0/503
goodness-of-fit on F^2	0.980
final *R* indices [$I > 2\sigma(I)$][a]	R1 = 0.0465, wR2 = 0.1104
R indices (all data)[a]	R1 = 0.0723, wR2 = 0.1233
largest diff peak and hole [e A^{-3}]	0.704 and −0.413

[a] $R1 = \Sigma||F_o| - |F_c||/\Sigma|F_o|$. $wR2 = [\Sigma w(F_o^2 - F_c^2)^2/\Sigma(w|F_o|^2)^2]^{1/2}$.

Table 4. Selected Bond Lengths [Å] and Angles [deg] for **2a**[a]

distance [Å]		angle [deg]	
Cu(1)−O(20)	1.945(3)	O(20)−Cu(1)−O(10)	88.99(15)
Cu(1)−O(10)	1.951(3)	O(20)−Cu(1)−O(5)#1	170.54(14)
Cu(1)−O(5)#1	1.962(3)	O(10)−Cu(1)−O(5)#1	97.54(14)
Cu(1)−O(5)	1.994(3)	O(20)−Cu(1)−O(5)	91.80(14)
Cu(1)−O(31)	2.241(3)	O(10)−Cu(1)−O(5)	175.32(14)
Cu(2)−O(41)	1.940(4)	O(5)#1−Cu(1)−O(5)	81.14(14)
Cu(2)−O(30)	1.969(4)	O(20)−Cu(1)−O(31)	90.07(15)
Cu(2)−O(5)	1.968(3)	O(10)−Cu(1)−O(31)	89.04(14)
Cu(2)−N(50)	1.995(4)	O(5)#1−Cu(1)−O(31)	96.84(14)
Cu(2)−O(11)#1	2.201(4)	O(5)−Cu(1)−O(31)	95.56(13)
O(5)−Cu(1)#1	1.962(3)	O(20)−Cu(1)−Cu(1)#1	131.67(11)
O(5)−H(5)	0.90(6)	O(10)−Cu(1)−Cu(1)#1	138.33(11)
Cu(1)−Cu(2)	3.3617(17)	O(5)#1−Cu(1)−Cu(1)#1	40.97(9)
Cu(1)−Cu(1)#1	3.0047(13)	O(5)−Cu(1)−Cu(1)#1	40.17(9)
Cu(1)−Cu(2)#1	3.3679(15)	O(31)−Cu(1)−Cu(1)#1	98.17(9)
Cu(2)−Cu(2)#1	6.0216(31)	O(41)−Cu(2)−O(30)	169.94(17)
		O(41)−Cu(2)−O(5)	94.40(16)
		O(30)−Cu(2)−O(5)	92.71(15)
		O(41)−Cu(2)−N(50)	85.94(18)
		O(30)−Cu(2)−N(50)	85.75(17)
		O(5)−Cu(2)−N(50)	169.16(16)
		O(41)−Cu(2)−O(11)#1	95.26(19)
		O(30)−Cu(2)−O(11)#1	91.21(16)
		O(5)−Cu(2)−O(11)#1	94.88(14)
		N(50)−Cu(2)−O(11)#1	95.88(17)
		Cu(1)#1−O(5)−Cu(2)	117.97(16)
		Cu(1)#1−O(5)−Cu(1)	98.86(14)
		Cu(2)−O(5)−Cu(1)	116.12(15)
		Cu(1)#1−O(5)−H(5)	112(3)
		Cu(2)−O(5)−H(5)	101(4)
		Cu(1)−O(5)−H(5)	111(4)

[a] Atoms generated by symmetry operator $-x + 1, -y, -z + 1$ are marked with #1.

forming two equal short bonds to two copper atoms, while the Cu−O bond to a third copper atom is longer by 0.03 Å. These O5 atoms are positioned about 0.6 Å above and below the plane defined by the corresponding three copper atoms. The fourth position is occupied by a hydrogen atom with the Cu−O5−H5 angles close to being tetrahedral. Both the temperature displacement parameter of that H atom being twice as high as that observed for O5 and the possibility of the intramolecular H bond formation to the noncoordinated O40 atom validate the assumption of the hydroxyl group presence.

There are two distinct groups of carboxylate anions. Two carboxylates are bidentate, and two others coordinate monodentately. However, the analysis of their environment reveals lack of additional electron density picks, which could be considered as protons. Instead, these oxygen atoms are stabilized by hydrogen bonds formed to a μ_3 hydroxyl group or to the protonated quinoline moiety. These interactions are not as strong as the coordination, and as a result, the respective C−O bonds in carboxylate groups are short. In **2a**, the carboxylate anions connect each copper atom with two others but never with their images generated by $(1 - x, -y, 1 - z)$ symmetry operator. Thus, they mediate interactions neither between two Cu1 nor between two Cu2 atoms. Cu1 and Cu1#1 are joined by two hydroxyl groups. However, there is no direct bridge between two outer Cu2 atoms located on the long axis of the diamond. Each of the copper atoms is coordinated monodentately by one carboxylate anion, O21 (Cu1) and O40 (Cu2), which subsequently create an intramolecular H bond to N60 of a quinH$^+$ cation and to O5 of the hydroxyl group, respectively. All copper atoms are coordinated in syn or syn/syn conformation, and the coordination produces some stress that results in Cu−O−C−O/O−C−O−Cu torsional angles differing slightly from 0°.

Comparison of 2a with 3, 4, and Little's Tetramer. The structure of **2a** is substantially different from our tetramers **3** and **4** and is topologically similar to Little's tetramer,[21] $[Cu_2(OH)(CF_3COO)_3(quin)_2]_2$. The bond lengths between copper atoms and μ_3 or μ_4 oxygen atoms are similar, and only two Cu−OH bonds in **2a** are longer by 0.03 Å than other Cu−O or Cu−OH distances. We observe that the average Cu−N bond lengths are longer by 0.02−0.03 Å in the μ_4-oxo tetramers **3** and **4** than in planar copper tetramers with the shortest distance found in $[Cu_2(OH)(CF_3COO)_3(quin)_2]_2$[21] This effect is even clearer in the case of axial Cu−O bonds, which are elongated by 0.1−0.15 Å in our tetrahedral tetramers. The differences observed for equatorial Cu−O bonds are not conclusive. We can state only that in **2a** they are 0.1−0.2 Å shorter than in three other tetramers discussed here. Thus, the main differences concern the ligand arrangement around the copper atoms. Tetramer **2a** is the only one among the compounds discussed here in which quinoline molecules are coordinated only to two outer copper atoms (Cu2 and symmetry-related Cu2#1).

Magnetic Susceptibility and EPR Spectra of the Tetrameric Complexes 3 and 4. The Heisenberg Hamiltonian that will be used in this paper for interpretation of the magnetic data for the tetramers is

$$\boldsymbol{H} = J_1\boldsymbol{S}_1\boldsymbol{S}_2 + J_2\boldsymbol{S}_3\boldsymbol{S}_4 + J_3(\boldsymbol{S}_1\boldsymbol{S}_3 + \boldsymbol{S}_1\boldsymbol{S}_4 + \boldsymbol{S}_2\boldsymbol{S}_3 + \boldsymbol{S}_2\boldsymbol{S}_4) \quad (1)$$

This Hamiltonian gives rise in a copper tetramer to one quintet ($S = 2$) level, three triplets ($S = 1$), and two singlet states ($S = 0$). The spin state energies can be easily evaluated:[22,23]

(22) Sinn, E. *Coord. Chem. Rev.* **1970**, *5*, 313–347.

$$E_{S=2} = J_1/4 + J_2/4 + J_3$$
$$E_{S=1} = J_1/4 - 3J_2/4,\ E'_{S=1} = -3J_1/4 + J_2/4,$$
$$E''_{S=1} = J_1/4 + J_2/4 - J_3$$
$$E_{S=0} = J_1/4 + J_2/4 - 2J_3,\ E'_{S=0} = -3J_1/4 - 3J_2/4 \quad (2)$$

In the μ_4-oxo tetramers there are no close contacts between copper atoms from different tetranuclear units, for example, in **3** the shortest such distance is Cu3−Cu1(0.5 + x,y,0.5 − z) 8.651(1) Å and Cu4−Cu2(0.5 − x,0.5 + y,z) 8.574(2) Å. The intertetramer interactions are thus not expected to affect the magnetic properties. The four copper ions in tetrameric molecules are joined by the central oxygen bridge and by six carboxylato bridges. The bridges Cu1−Cu2 and Cu3−Cu4 are symmetric (see the structure description and Figure 5), while other four carboxylato bridges are asymmetric. Also, the Cu1−O5−Cu2 and Cu3−O5−Cu4 angles of 119° are much larger than other four Cu_i−O5−Cu_j angles (102°, 104°, 107°, 107°). Thus, $J_1 = J_2$ was set in the Hamiltonian (eq 1).

Strong increase of the effective magnetic moment (related to four Cu(II) ions, Figure 3) with decreasing temperature is an indication of ferromagnetic coupling in the system. Considering the magnetic moment of ca. 5.1 μ_B at the maximum, the population of the $S = 2$ ground state must be complete, while the magnetic moment decrease at the lowest temperatures is caused by the combined zero-field and Zeeman splitting of the $S = 2$ state becoming comparable to kT.

To reproduce the magnetic moment decrease at the lowest temperatures, it is necessary to take the Hamiltonian of the system as a sum of the isotropic part (eq 1) and the part expressing the anisotropic metal−metal interactions and the Zeeman interaction in the tetramer:

$$\boldsymbol{H}_{\text{aniso}} = \sum_{i=1}^{3}\sum_{j=i+1}^{4} \boldsymbol{S}_i\{\boldsymbol{D}_{ij}\}\boldsymbol{S}_j + \mu_B \sum_{k=1}^{4} B\{\boldsymbol{g}_k\}\boldsymbol{S}_k \quad (3)$$

where $\{\mathbf{D}_{ij}\}$ is a zero-field splitting tensor representing the sum of the anisotropic exchange and dipole−dipole interactions between Cu_i and Cu_j. $\{\mathbf{g}_k\}$ is the **g**-tensor of Cu_k. The orientations of $\{\mathbf{g}_k\}$ (particularly of their z components) are predictable from the geometric structure, but the orientations of the $\{\mathbf{D}_{ij}\}$ tensors are not. For the powder magnetic susceptibility calculation it is sufficient to assume isotropic {g} on each copper atom and to take into account the zero-field splitting of only the ground $S = 2$ state. In this way, $J_1 = J_2$ and J_3 were fitted while the D and E parameters for $S = 2$ were fixed as found from EPR (see the EPR section). The average g value was allowed to vary. The 16 by 16 Hamiltonian matrix was diagonalized to find energies E_i and the molar magnetic susceptibility was expressed as

$$\chi = -\frac{N}{B}\frac{\sum_{i=1}^{16}\frac{\partial E_i}{\partial B}\exp(-E_i/kT)}{\sum_{i=1}^{16}\exp(-E_i/kT)} \quad (4)$$

The derivatives $\delta E_i/\delta B$ were evaluated numerically by diagonalizing $\boldsymbol{H} + \boldsymbol{H}_{\text{aniso}}$ at magnetic fields 1 Gauss above and

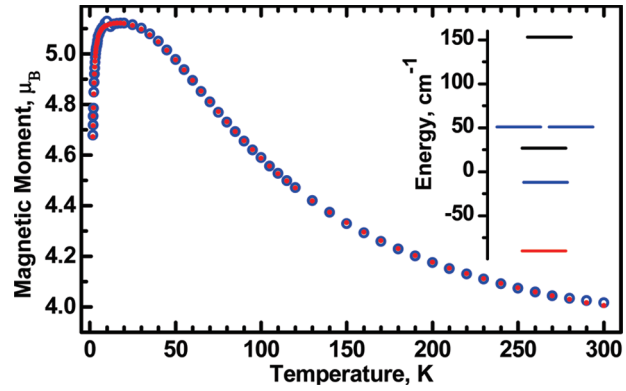

Figure 3. Magnetic moment (related to four Cu ions) for the benzene solvate **4**. Blue circles are experimental values measured at 5000 G; red dots are calculated with $g_{\text{average}} = 2.09$, $J_1 = -102$ cm^{-1}, $J_2 = -39$ cm^{-1}, $D_{S=2} = -0.89$ cm^{-1}, $E_{S=2} = -0.011$ cm^{-1}. Inclusion of the zfs terms in addition to the Zeeman term is necessary for correct magnetic moment evaluation at temperatures below 10 K. The inset shows spin state energies. Red, blue, and black lines represent the quintet, triplets, and singlets, respectively.

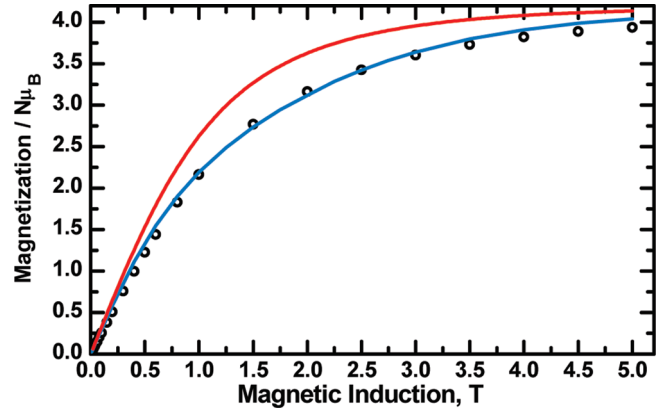

Figure 4. Magnetization of **4**, in multiples of $N\mu_B$, measured at 1.8 K (black circles). The theoretical saturation value equals gS. Blue line: magnetization calculated as $\chi B/N\mu_B$ with inclusion of the zero-field splitting using χ from eq 4. Red line: calculated from the Brillouin function including only the Zeeman term: $M = -\mathbf{g}\Sigma_{m=-2}^{2} m \exp(-g\boldsymbol{\mu}_B Bm/kT)/\Sigma_{m=-2}^{2}\exp(-g\boldsymbol{\mu}_B Bm/kT)$. $\mathbf{g} = 2.09$ was used in both calculations.

1 Gauss below the working magnetic field of the magnetometer, $B = 5000$ G. Inclusion of the D and E parameters for $S = 2$ spin state in addition to the Zeeman term dramatically improved the magnetic moment fitting for **3** and **4** at temperatures below 10 K (Figure 3), and that effect is even more visible in the magnetization measured at 1.8 K (Figure 4). The fitting resulted in $J_1 = J_2 = -97(3)$ cm^{-1}, $J_3 = -37(1)$ cm^{-1} for **3** and $J_1 = J_2 = -102(2)$ cm^{-1}, $J_3 = -39(1)$ cm^{-1} for **4**.

To avoid the complexity of the above treatment, one can limit the data set to fit only susceptibilities above ~20 K. The isotropic Hamiltonian (eq 1) is then acceptable, and susceptibility can be calculated from the more commonly known formula

$$\chi = \frac{Ng^2\mu_B^2}{3kT}\frac{\sum_{i=1}^{6}(2\boldsymbol{S}_i + 1)(\boldsymbol{S}_i + 1)\boldsymbol{S}_i \exp(-E_i/kT)}{\sum_{i=1}^{6}(2\boldsymbol{S}_i + 1)\exp(-E_i/kT)} \quad (5)$$

where the summations run over two singlet, three triplet, and one quintet state whose energies are given by eqs 2. When doing so, essentially the same exchange integrals as above are found.

(23) Buvaylo, E. A.; Kokozay, V. N.; Vassilyeva, O.Yu.; Skelton, B. W.; Jezierska, J.; Brunel, L. C.; Ozarowski, A. *Inorg. Chem.* **2005**, *44*, 206–216.

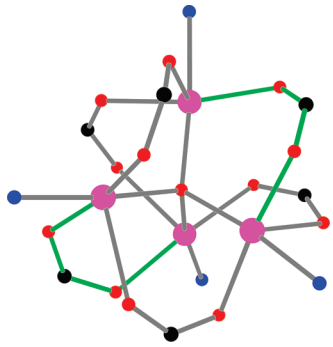

Figure 5. Copper coordination and the system of bridges in **3** and **4**. Purple = Cu, blue = N, red = O, black = C. Two carboxylate bridges (marked in green) join an equatorial position of one copper with an equatorial position of another copper atom, while the four remaining carboxylates join an equatorial position of one copper atom with an axial position of another.

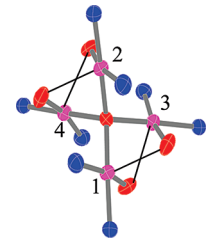

Figure 6. Copper coordination and the system of bridges in $[Cu_4(\mu_4\text{-}O)(bahped)_2](ClO_4)_2$. Black lines indicate the oxygen atoms bridging an equatorial position of one copper atom with an axial position of another copper atom in the 1-3 and 2-4 copper pairs. The diagram was generated from cif data in ref 16.

Both the large ferromagnetic values of the exchange integrals and the large difference between them appear surprising, as other μ_4-oxo copper tetramers are antiferromagnetic.[16,18,24−29] The fitted $g_{average}$ value of 2.09 was somewhat smaller than found from EPR (2.14). Such discrepancies are common.

Estimation of the Exchange Integrals by DFT Calculations. "Broken symmetry" calculations were attempted by using the free software package ORCA developed by F. Neese.[30] For that purpose the tetrameric molecule was simplified by placing pyridine molecules on the quinoline positions. That transformation was accomplished by inserting hydrogen atoms on the vectors joining appropriate carbon atoms in the quinoline rings. Coordinates from the X-ray structure of **3** were used for all other atoms, and the structure was not optimized by DFT. Six separate calculations were performed. In each of them two of the four copper ions were replaced by zinc, thus leaving a system with only one exchange interaction between the remaining two copper ions. The calculation utilized the basis Ahlrichs-VDZ[31] and polarization functions from the Ahlrichs polarization basis.[30] In each case the exchange integrals were calculated according to the convention[32] $J = 2(E_{HS} - E_{BS})/(S_{HS}(S_{HS} + 1))$, where HS and BS denote the high-spin state and the broken-symmetry state, respectively. This convention is equivalent to that of ref 33 where exchange coupling in copper paddlewheel dimers was studied by DFT. The original formula for J from ORCA, which uses the exchange Hamiltonian $\mathbf{H} = -2JS_aS_b$, was converted to the notation used in this paper by multiplying it by −2. Our calculations resulted in $J_{Cu1-Cu2} = -108$ (119°), $J_{Cu3-Cu4} = -122$ (119°), $J_{Cu1-Cu3} = -56$ (102°), $J_{Cu1-Cu4} = -82$ (104°), $J_{Cu2-Cu3} = -55$ (107°), and $J_{Cu2-Cu4} = -33$ cm^1 (107°). Angles $Cu_i-O5-Cu_j$ are given in parentheses. Two interactions, $J_{Cu1-Cu2}$ and $J_{Cu3-Cu4}$, involve the symmetric carboxylato bridges, and their average of -115 cm^{-1} can be considered to represent $J_1 = J_2$ in the Hamiltonian (eq 1), while the average value of -56 cm^{-1} for the other four, which are transmitted through the asymmetrically bound carboxylate bridges, represents J_3. The calculations are in surprisingly good agreement with the results of magnetic susceptibility fitting; the exchange interactions are indeed expected to be strongly ferromagnetic and the predicted $J_{1,2}/J_3$ ratio is large. It is however surprising that the ferromagnetic interactions are both calculated and found experimentally with the CuOCu angles as large as 119°. Bera et al. reported the copper tetramer $[Cu_4(\mu_4\text{-}O)(bahped)_2](ClO_4)_2$, which they described as containing only a μ_4-oxo bridge without any bridging ligand along the six tetrahedral edges.[16] However, there are four bridges in that structure, in which an equatorial oxygen atom of one copper is 20° away from the axial position of another copper atom at a distance 2.47 Å (Figure 6). The magnetic properties were interpreted using the Heisenberg Hamiltonian with three pairs of equal J values, J_1, J_2, and J_3. (Note that eqs 2 are not applicable to this case). $J_1 = J_2 = 120$ cm^{-1} was found (converted to our notation), whereas J_3 was undetermined but also antiferromagnetic.[16] We performed broken symmetry calculations for this complex in the same way as above after replacing two copper atoms by zinc and shortening the CH_3 groups in bahped to H. The results are $J_{12} = J_{34} = +127$ (131°), $J_{13} = J_{24} = -61$ (93°), $J_{14} = J_{23} = -49$ (108°). The $Cu-\mu_4O-Cu$ angles are in parentheses. The stronger ferromagnetic interactions are calculated for two copper pairs, 1-3 and 2-4 for which the μ_4-oxo angle is the smallest. The copper atoms in each of these two pairs are joined by two asymmetric phenoxo-bridges in addition to the μ_4-oxo bridge. The μ_4-oxo bridges 1-2 and 3-4 with the most obtuse angle transmit strong antiferromagnetic interactions resulting in the diamagnetic ground state for the complex, in agreement with the experiment, although only $J_{12} = J_{34}$ are close to those determined in ref 16.

Some control calculations have also been performed. Thus, we found by ORCA $J = 380$ cm^{-1} for **1**, while the experimental value is 310−340 cm^{-1} depending on the method used (magnetic susceptibility versus EPR intensity measurements, see

(24) Lines, M. E.; Ginsberg, A. P.; Martin, R. L. *Phys. Rev. Lett.* **1972**, *28*, 684–687.
(25) Mukherjee, S.; Weyhermüller, T.; Bothe, E.; Wieghardt, K.; Chaudhuri, P. *Eur. J. Inorg. Chem.* **2003**, 863–875.
(26) Atria, A. M.; Vega, A.; Contreras, M.; Valenzuela, J.; Spodine, E. *Inorg. Chem.* **1999**, *38*, 5681–5685.
(27) Chen, L. Q.; Breeze, S. R.; Rousseau, R. J.; Wang, S. N.; Thompson, L. K. *Inorg. Chem.* **1995**, *34*, 454–465.
(28) Black, T. D.; Rubins, R. S.; De, D. K.; Dickinson, R. C.; Baker, W. A. *J. Chem. Phys.* **1984**, *80*, 4620–4624.
(29) Buluggiu, E. *J. Chem. Phys.* **1986**, *84*, 1243–1246.
(30) Neese, F. *ORCA*, an ab initio, Density Functional and Semiempirical Program Package, Version 2.6−35, 2008; Universität Bonn: Bonn, Germany; free download from http://www.thch.uni-bonn.de/tc/orca/, registration required.
(31) (a) Schaefer, A.; Horn, H.; Ahlrichs, R. *J. Chem. Phys.* **1992**, *97*, 2571. (b) Ahlrichs et al. Unpublished work. (c) The Ahlrichs auxiliary basis sets were obtained from the TurboMole basis set library under ftp.chemie.uni-karlsruhe.de/pub/jbasen. (d) Eichkorn, K.; Treutler, O.; Ohm, H.; Haser, M.; Ahlrichs, R. *Chem. Phys. Lett.* **1995**, *240*, 283–289. (e) Eichkorn, K.; Weigend, F.; Treutler, O.; Ahlrichs, R. *Theor. Chem. Acc.* **1997**, *97*, 119–124.
(32) A. Bencini, A.; Gatteschi, D. *J. Am. Chem. Soc.* **1986**, *108*, 5763–5771.
(33) Rodriguez-Fortea, A.; Alemany, P.; Alvarez, S.; Ruiz, E. *Chem.—Eur. J.* **2001**, *7*, 627–637.

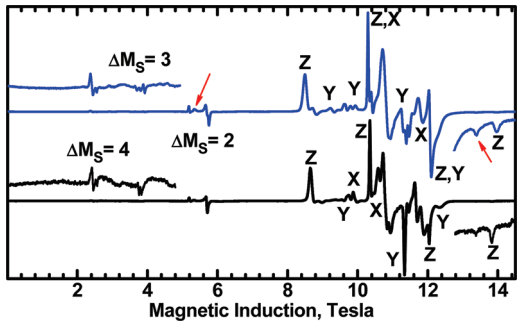

Figure 7. EPR spectra of **3** (bottom) and of **4** (top) at 15 K and 324 GHz. The molecular orientations for the resonance lines are marked by X, Y and Z. The distance between the outer Z lines is 5.48 T in **4** and 5.18 T in **3**. Arrows indicate signals due to frozen oxygen ($S = 1$, $g_{iso} = 2$, $D = 3.57$ cm^{-1}) that is frequently observed below $T = 30$ K.[48]

below). For dimer **2** with quinoline shortened to pyridine the calculated J was 350 cm^{-1}, while 310 cm^{-1} has been reported.[6] The calculated J values appear to be imperfect but sensible and give us more confidence in our results obtained for **3**. It should be mentioned that the exchange coupling in tetranuclear copper cubanes has been studied by using DFT without resorting to the copper substitution by zinc.[33,34]

EPR Spectra of the μ_4-oxo Tetramers 3 and 4 (Figure 7). Both **3** and **4** exhibited at low temperatures and high microwave frequencies complicated and very well resolved EPR spectra characteristic of $S = 2$ spin state. The resolution deteriorated fast with temperature above 60 K and no spectra of excited triplet states were observed, which is rather typical.[23,28,29] Both triplet and quintet state spectra in a tetrameric copper complex were observed in ref 35.

The spin Hamiltonian used to describe the quintet-state spectra was

$$H = \mu_B \mathbf{B}\mathbf{g}\mathbf{S} + D\{S_z^2 - S(S+1)/3\} + E(S_x^2 - S_y^2) + B_4^0 O_4^0 + B_4^2 O_4^2 + B_4^4 O_4^4 \quad (6)$$

Expressions for the fourth-rank spin operators O_4^i are given for example in ref 36. The spin Hamiltonian parameters were found by least-squares fitting of the resonance field versus microwave frequency dependencies measured over a wide frequency range (Figure 8 and Figure S2, Supporting Information). The fitting required usage of the fourth-order terms B_4^i. The fit was quite good, and the resonance fields for both the "allowed" transitions and the "forbidden" transitions with $\Delta M_S = 2$, 3, and 4 were very well simulated.

The simulation of the powder spectra was less satisfactory, as far as the relative intensities are concerned. One of the reasons for the problems may be the very peculiar line width pattern. The linewidths vary with orientation and also are different for various transitions at an orientation. For example, the outer Z lines corresponding to the transitions between the M_S states $2 \leftrightarrow 1$ and $-2 \leftrightarrow -1$ are much broader than the inner $1 \leftrightarrow 0$ and $-1 \leftrightarrow 0$ transitions indicating a "D-strain" in the system. Powder

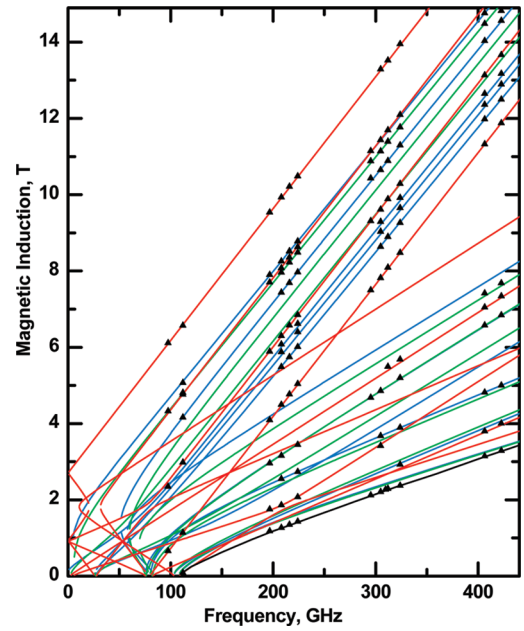

Figure 8. Resonance field versus frequency dependences observed for **4** at 15 K. Black triangles are the experimental points. The green, blue, and red lines were calculated for the magnetic field oriented along the molecular x, y, and z axes, respectively, assuming $S = 2$ with the spin Hamiltonian parameters from Table 5. The group of lines with steepest slope corresponds to the "allowed" transitions $\Delta M_S = 1$, while the slopes of the $\Delta M_S = 2$, 3, and 4 transitions are progressively smaller. The black line near the bottom represents the "minimum magnetic field", which is due to an off-axial $\Delta M_S = 4$ turning point with an effective magnetic field orientation $\Theta = 54°$, $\Phi = 45°$.

simulations improved somewhat when strain was taken into account. With the magnitudes of $J_{1,2}$ and J_3 as found from the magnetic susceptibility, no EPR transitions are possible between the ground $S = 2$ state and the excited states. No resonances within the excited states were identified with the possible exception of a broad line in the center of the spectra of both **3** and **4** (Figure 7). X-ray structures of both tetramers reveal high dynamics and disorder, and it may be possible that molecules freeze into a number of conformations with slightly different EPR parameters. Also, the zero-field splitting tensor is likely to be noncoaxial with the **g** tensor and the Dzialoshinskii−Moriya interactions may be operative in the system where copper atoms are not related by the inversion center[24] but both effects cannot be further investigated in the absence of large single crystals suitable for high-field EPR. Nevertheless, considering the goodness of the fit shown in Figures 7 and S2 in Supporting Information, and the fact that the resonance fields for the "forbidden" lines were well reproduced, we conclude that the **g** components as well as the magnitudes of D and E have been determined with good certainty. The spin Hamiltonian parameters for **3** and **4** are given in Table 5. The benzene solvate **4** exhibits larger D than **3**, while E is smaller in **4** than in **3.** The **g** components are equal for both complexes within the error limits.

EPR spectra of copper tetramers have been occasionally reported, but successful interpretations are very rare.[23,28,29,35] Black et al.[28] investigated a highly symmetric tetranuclear copper triphenylphosphine oxide complex $Cu_4OCl_6(TPPO)_4$ and interpreted its EPR spectra by using a spin Hamiltonian containing only the Zeeman interaction and the fourth-order cubic zero-field splitting term $B_4(O_4^0 + 5O_4^4)$ with $B_4 = 0.0044$ cm^{-1}. In our case, large D and E parameters were found in

(34) (a) Ruiz, E.; Alvarez, S.; Cano, J.; Polo, V. *J. Chem. Phys.* **2005**, *123*, 164110. (b) Tercero, J.; Ruiz, E.; Alvarez, S.; Rodriguez-Fortea, A.; Alemany, P. *J. Mater. Chem.* **2006**, *16*, 2729–2735.
(35) Prins, R.; Degraaff, R. A. G.; Haasnoot, J. G.; Vader, C.; Reedijk, J. *J. Chem. Soc. Chem. Commun.* **1986**, *18*, 1430–1431. Mialane, P.; Duboc, C.; Marrot, J.; Rivière, E.; Dolbecq, A.; Sécheresse, F. *Chem.—Eur. J.* **2006**, *12*, 1950–1959.
(36) Abragam, A.; Bleaney, B. In *Electron Paramagnetic Resonance of Transition Ions*; Dover Publications, Inc.: New York, 1986.

Table 5. Quintet-State ($S = 2$) EPR Parameters[a] for Tetrameric Complexes **3** and **4**

	g_x	g_y	g_z	D, cm^{-1}	E, cm^{-1}	B_4^0, cm^{-1}	B_4^2, cm^{-1}	B_4^4, cm^{-1}
3	2.168(5)	2.173(5)	2.066(1)	−0.827(2)	−0.114(4)	0.000(1)	−0.0114(4)	0.0012(4)
4	2.169(3)	2.175(1)	2.067(1)	−0.875(1)	−0.049(1)	0.000(3)	−0.009(1)	−0.006(1)

[a] The fitting procedure and estimation of parameter errors are explained in Supporting Information; see Figure S2.

addition to the fourth-order terms. This is not surprising because the molecular symmetry of **3** and **4** is lower than of the TPPO complex. In the latter, the energy difference between the lowest and the highest level of the quintet state at the zero magnetic field is 0.5 cm^{-1}, while it is about 3.5 cm^{-1} in **3** and **4**. $D = -0.353$ cm^{-1} was found in a ferromagnetic tetrameric copper cubane[23] causing an overall zero-field splitting of 1.4 cm^{-1}. The D and E parameters in **3** and **4** are exceptionally large and must be due to the anisotropy of the exchange interactions, since the dipolar contribution is negligible (see below). It has to be emphasized here that the EPR spectra of **3** and **4** as well as of **3a** (below) could not be studied using standard X-band or even Q-band EPR because of the large zero-field splitting.

The **g** values are very different from those expected for a mononuclear Cu(II) with tetragonal symmetry ($\mathbf{g}_z \approx 2.2-2.4$; $\mathbf{g}_{x,y} \approx 2.02-2.08$),[1,3,8,36] which is the result of the single ion $\boldsymbol{g}$ tensors not being aligned in the tetranuclear system. There is no experimental way to determine the $\boldsymbol{g}$ components of individual ions in an exchange coupled system. It is possible, however, to use the molecular structure and simple assumptions about Cu(II) $\boldsymbol{g}$ tensors to explain the results as follows. Using the X-ray structure of **3**, the coordinate systems for each copper ion were set up with the z axis for each copper ion assumed perpendicular to the least-squares plane of its equatorial ligands. The x axis was perpendicular to z and to the vector joining Cu and the central oxygen and finally y was perpendicular to both x and z. The tensors for the four copper atoms, $\boldsymbol{g}_1-\boldsymbol{g}_4$, were assumed axial, i.e., $g_x = g_y$, and equal to each other, except for their orientation in space. The $\boldsymbol{g}_2$, $\boldsymbol{g}_3$, and $\boldsymbol{g}_4$ tensors were rotated to the system of coordinates of $\boldsymbol{g}_1$, summed according to formula 7 below and diagonalized to obtain the main values and main axes of $\boldsymbol{g}$ in the $S = 2$ state.[37]

$$\boldsymbol{g}_{S=2} = (\boldsymbol{g}_1 + \boldsymbol{g}_2 + \boldsymbol{g}_3 + \boldsymbol{g}_4)/4 \tag{7}$$

When $g_z = 2.31$ was assumed implying that $g_x = g_y = 2.05$ (the average g must be equal to that found from EPR for $S = 2$) then the resulting three g components for $S = 2$ were 2.166, 2.180 and 2.065, resembling very closely the values determined from EPR. $g_{x,y} = 2.05$ and $g_z = 2.31$ are reasonable for a copper ion having three oxygen atoms and one nitrogen in its equatorial plane and may be used as estimates of the single-ion g values in **3**. The g-tensor main axis corresponding to $g = 2.065$ lies along the approximate S_4 axis of the distorted Cu_4 tetrahedron, at a 1.2° angle from the O5−C102 vector.

Dipolar Contribution to the ZFS Parameters. Formula 3 in ref 38 was used to calculate dipolar tensors for each of the six magnetic dipole−dipole interactions in the tetrameric system:

$$D_{\alpha\gamma} = g_{m\alpha}\{\sum_i g_{ni} d_{\gamma i}(d_{\alpha i} - 3\sigma_\alpha \sum_j d_{ji}\sigma_j\}\mu_B^2/r^3 \tag{8}$$

$g_{m\alpha}$ and g_{ni} are the g_x, g_y, and g_z components for two ions "m" and "n" in the interacting pair, $d_{\gamma i}$ are elements of the matrix that transforms $\boldsymbol{g}_n$ axes into the $\boldsymbol{g}_m$ axes, and σ_α are the direction cosines of the vector $\boldsymbol{r}$ joining the atoms "m" and "n", expressed in the $\boldsymbol{g}$ axes of atom "m". All six tensors were then transformed into a common system of coordinates and added according to formula (9) that relates the zero-field splitting tensor components expressed in terms of the spins of separate ions and those appropriate for the total spin $S = 2$:[37]

$$D_{ij}(S = 2) = \frac{1}{12}\sum_k D_{ij}^{(k)} \tag{9}$$

where k runs over the six interactions 1-2, 1-3, 1-4, 2-3, 2-4, and 3-4.

The resulting matrix was diagonalized yielding $D_{xx} = -0.0125$ cm^{-1}, $D_{yy} = 0.0097$ cm^{-1}, $D_{zz} = 0.0019$ cm^{-1}. Application of the relations between D, E, and the ZFS tensor components

$$D = (2D_{zz} - D_{xx} - D_{yy})/2, \quad E = (D_{xx} - D_{yy})/2 \tag{10}$$

yielded finally $D_{\text{dipole}}(S = 2) = -0.0183$ cm^{-1}. This is only about 1/45 of D as determined from EPR, indicating an overwhelming contribution of the anisotropic exchange interactions to the zero-field splitting in the tetranuclear molecule. Calculated $E_{\text{dipole}}(S = 2)$ is 0.0039 cm^{-1}, 29 times less than the experimental E value in **3**.

Magnetic Properties of the Blue Complex 2a. This blue substance is different from the blue product **3a** forming from the tetramer and exhibits no discernible EPR spectrum at any frequency and temperature, which appears to be due to enormous line width. Magnetic susceptibility of the blue compound was measured revealing antiferromagnetic exchange interactions which were much weaker than in the original yellow-green dimer **2**. Before fitting, the monomer susceptibility was subtracted from experimental data. The monomer susceptibility was calculated from

$$\chi_{\text{mono}} = (Ng\mu_B/2B)(x - 1/x)/(x + 1/x) \tag{11}$$

where $x = \exp(g\mu_B B/2kT)$ and B is the magnetic induction of the magnetometer (5000 G).

Using the Curie law to calculate the monomer susceptibility at the lowest temperatures would not be proper because the Zeeman splitting (~0.47 cm^{-1} at 5000 G) is comparable to kT (1.4 cm^{-1} at 2 K). The procedure was only partially successful as the remaining susceptibility did not approach zero at the lowest temperatures in the manner the antiferromagnetic susceptibility should (Figure 9). The effect of the monomer contribution removal on the susceptibility at higher temperatures was very small, and data below 20 K were subsequently not fitted. Judging from the molecular structure (Figures 2 and 10), the Hamiltonian (eq 1) with all J_1, J_2, and J_3 being different is appropriate for fitting of the magnetic susceptibility.

(37) Bencini, A.; Gatteschi, D. In *EPR of Exchange Coupled Systems*; Springer Verlag: Berlin, Heidelberg, 1990; p 118.
(38) Carr, S. G.; Smith, T. D.; Pilbrow, J. R. *J. Chem. Soc., Faraday Trans. 2* **1974**, *70*, 497–511.

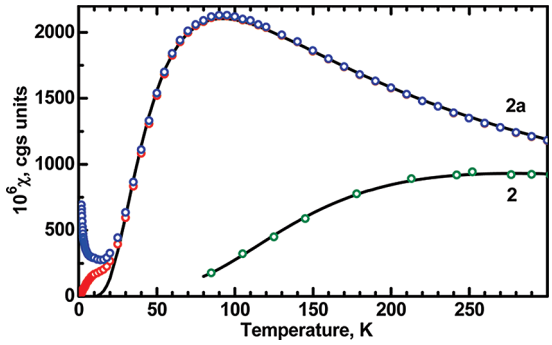

Figure 9. Magnetic susceptibility (per 1 Cu) of the blue tetramer **2a**. Blue circles = original data points; red circles = susceptibility after subtraction of 0.28% of monomeric contamination. Black line was calculated with $J_1 = J_2 = 0$, $J_3 = 81$ cm^{-1}, $g = 2.17$ (see text). Green circles are the data for green dimer **2** from ref 6. Solid line was calculated for a dimer with $J = 310$ cm^{-1} and $g = 2.27$.[6]

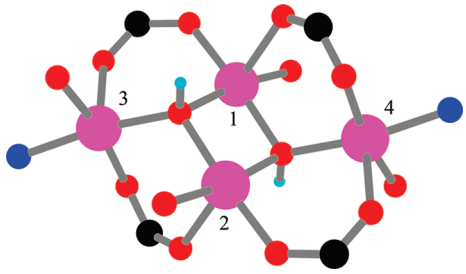

Figure 10. Copper coordination and the bridge system in **2a**.

J_2 should be small because there is no direct bridge between Cu3 and Cu4 and was fixed to zero. Basing on results of ORCA calculations for this compound the J_1 (Cu1−Cu2 in Figure 10) value was also fixed to zero (see below). The fit then resulted in $J_3 = 81$ cm^{-1}, $g = 2.17$ (g could not be determined independently because **2a** exhibits no EPR). The model with only four equal exchange integrals in the ring containing four copper ions appears to be fully adequate.

ORCA calculations were performed as described above, i.e., by replacing two copper atoms by zinc and evaluating the exchange integral between the remaining two copper atoms. Antiferromagnetic J values were found: the interaction between two closest copper atoms J_{12} was the smallest, 3.5 cm^{-1}, followed by four 12 cm^{-1} interactions in the ring Cu1−Cu3−Cu2−Cu4, while $J_{34} = 25$ cm^{-1} was the largest. A small J_{12} magnitude can be rationalized since the Cu1−O−Cu2 angle of 98.6° lies on the borderline 97−98° separating the ferromagnetic and antiferromagnetic interactions in dihydroxo-bridged copper dimers.[39] As for J_{34}, it is not clear to us whether a "direct" Cu3−Cu4 exchange should be considered at all when the exchange pathways involve the inner Cu1 and Cu2 atoms. The large value of J_{34} derived from DFT may be associated with the calculation method, in which the intervening Cu1 and Cu2 atoms were replaced by zinc. In this context it is worth mentioning that an exchange integral of 35 cm^{-1} was found experimentally in a dimer containing two Cu ions bridged by two OZnO groups.[40]

(39) Crawford, V. H.; Richardson, H. W.; Wasson, J. R.; Hodgson, D. J.; Hatfield, W. E. *Inorg. Chem.* **1976**, *15*, 2107–2110.
(40) Buvaylo, E. A.; Kokozay, V. N.; Vassilyeva, O.Yu.; Skelton, B. W.; Jezierska, J.; Brunel, L. C.; Ozarowski, A. *Chem. Commun. (Cambridge)* **2005**, *39*, 4976–4978.

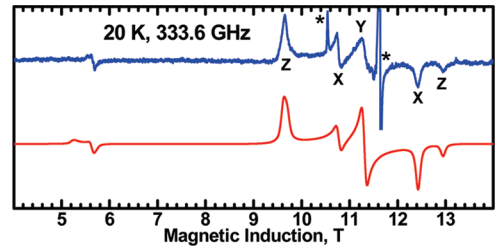

Figure 11. Blue: EPR spectrum of **3a**. Asterisks indicate resonances due to a monomeric copper species. Sharp "perpendicular" part of the monomer signal is cut off to make the triplet spectrum better visible. Red: Spin-triplet spectrum simulated with $g_x = 2.049$, $g_y = 2.263$, $g_z = 2.112$, $D = -1.636$ cm^{-1}, $E = -0.0187$ cm^{-1}.

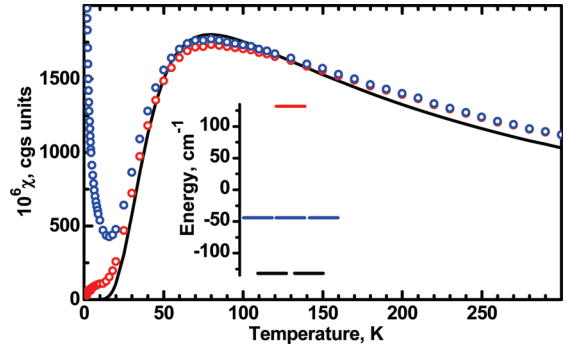

Figure 12. Magnetic susceptibility of **3a** (blue circles). Red circles: susceptibility after subtraction of 0.93% of monomeric impurity. Solid line was calculated with $J_1 = J_2 = J_3 = 88$ cm^{-1} and $g_{average} = 2.14$. The inset shows energies of the spin states. Red, blue, and black lines represent the quintet, triplets, and singlets, respectively.

Blue Product (3a) Forming from the Tetramer (3). Samples of tetramer **3** kept for several days in humid air changed color from green to blue and increased in weight by 3%. The blue compound exhibited EPR spectra characteristic of a triplet state with $g_x = 2.049$, $g_y = 2.263$, $g_z = 2.112$, $D = -1.636$ cm^{-1}, $E = -0.019$ cm^{-1}. A weak spectrum of monomeric copper(II) with $g_x = g_y = 2.048$, $g_z = 2.263$ was also observed (Figure 11). No crystals suitable for the structure determination could be obtained.

This spectrum broadened very quickly with increasing temperature and was not seen above 80 K. The triplet spectrum also disappeared below 10 K, leaving behind only the monomer signals.

Magnetic susceptibility of the blue compound in Figure 12 shows an antiferromagnet contaminated by a monomer. Before fitting, the monomer susceptibility was subtracted from experimental data as described above. A 0.93% monomer content can be estimated from the susceptibility over the range 2−10 K; this was subtracted from all experimental points and data below 20 K were subsequently not fitted. The monomer was also seen in EPR (Figure 11). The susceptibility has a maximum at $T_{max} = 80$ K. If the complex were a dimer then the J value would be $J = 1.6\ kT_{max}$ or 90 cm^{-1}, but then the susceptibility would have to be much higher (2600×10^{-6} cgs emu at the maximum with $g = 2.1$) than observed (1700×10^{-6}), and the dimer model has to be rejected, although this compound of unknown structure exhibits triplet EPR spectra.

Fitting under assumption that the complex was still tetrameric was more successful (Figure 12). The relatively best fit was achieved with all six J values equal to 88 cm^{-1} (by setting $J_1 = J_2 = J_3$ in eqs 2) and with fixed $g_{average} = 2.14$, as found from EPR. Fitting the magnetic susceptibility of an antiferro-

magnetic tetramer is not easy and results less satisfactory than in Figure 12 are commonly seen in the literature. This blue complex thus appears to be tetranuclear but with drastically altered magnetic properties compared to its parent green tetramer. The exchange interactions are now antiferromagnetic and the ground state is a singlet with $S = 0$. The observed triplet spectrum comes from an excited $S = 1$ state lying about 88 cm^{-1} higher. Crystal structures of **2a**, **3**, and **4** show high flexibility of the carboxylates: they may be bridging, chelating, or dangling while IR spectra indicate that the μ_4-oxo bridge in the blue complex under discussion is retained. While it is clear that the bridge structure must have changed, no sufficient evidence was gathered in this case to propose a structure for this species.

Magnetic and EPR Properties of the Binuclear Complexes. $[Cu(CF_3COO)_2 \cdot (CH_3CN)]_2$ (1). Magnetic susceptibility of **1** has not been reported[5] and was therefore measured here (Figure S5, Supporting Information). The exchange integral magnitude J, corresponding to the spin Hamiltonian

$$\boldsymbol{H} = J\boldsymbol{S}_1\boldsymbol{S}_2 \qquad (12)$$

was found from least-squares fitting. With $g_{average}$ fixed at 2.18 as determined by EPR, $J = 312$ cm^{-1} was obtained. The temperature-independent paramagnetism (TIP) for copper was fixed at 60×10^{-6} cgs units.

A relatively high content of paramagnetic impurity (ca. 3.4%) was also revealed. This is likely associated with the hygroscopicity of this substance. Measurements of the single-crystal EPR signal intensity was also performed to find J independently. The high-field "perpendicular" transition centered at 4910 G at the X-band frequency was used for this purpose.

The EPR signal intensity was fitted with the equation

$$I = (C/T)\exp(-J/kT)/(1 + 3\exp(-J/kT)) \qquad (13)$$

where C is a proportionality constant. The EPR intensity is proportional to the magnetic susceptibility (taking $C = Ng^2\mu_B^2/k$ converts eq 13 to the magnetic susceptibility referred to one Cu atom) but is not affected by paramagnetic contaminants (which typically give signals close to $g = 2$ or 3400 G in X-band EPR), nor does it require correction for ligand diamagnetism and temperature independent paramagnetism of copper. However, the procedure is quite cumbersome owing to a need of single crystal measurements followed by double integration of the spectra (see Figures S5, S5a in Supporting Information). Fortunately, **1** forms very large crystals of high quality exceptionally easily. J of 339(8) cm^{-1} obtained in this way was in reasonable agreement with the magnetic susceptibility data.

EPR Spectra and the Sign of D in Dimeric Complexes 1 and 2. EPR spectra of binuclear complexes are described by the spin Hamiltonian

$$\boldsymbol{H} = \mu_B\boldsymbol{B}\boldsymbol{g}\boldsymbol{S} + D\{\boldsymbol{S}_Z^2 - S(S+1)/3\} + E(\boldsymbol{S}_x^2 - \boldsymbol{S}_y^2) \qquad (14)$$

Although positive sign of the zero-field splitting parameter D in binuclear copper carboxylates has been reported in literature,[41−43] a recent high-field EPR study of copper acetate monohydrate dimer and its pyrazinate analogue showed that D is in fact negative.[8] High-field EPR measurements have thus been performed in this work on single crystals of **1** and **2** to determine the sign of D. Powder EPR spectra of antiferromagnetic dimers are not suitable for that purpose.[8] The EPR

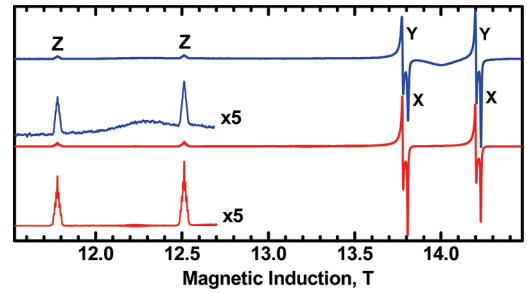

Figure 13. Powder EPR spectrum of **1** at 80 K and 406.4 GHz. Blue: experimental; red: simulated with parameters from Table 6. Broad signals of a monomeric impurity are seen between the $S = 1$ state signals. Hyperfine structure due to two copper nuclei ($A_z = 67 \times 10^{-4}$ cm^{-1}, half of that expected for a monomeric Cu complex with four equatorial oxygen atoms) appears on the "Z" resonances.

parameters for **1** and **2** found at 50−80 K from the high-field EPR spectra (Figures 13 and S4 in Supporting Information) are shown in Table 6. $|D|$ is substantially larger than in nonhalogenated copper carboxylates (~0.33 cm^{-1}, Table 6). Single-crystal spectra were recorded with $\nu = 432$ GHz at 80 and 50 K. The triplet state population at 50 K is only about 2×10^{-4}, and hyperfine splitting due to two copper nuclei clearly appears because the paramagnetic molecules are diluted in the diamagnetic bulk of the sample. Since the spin Hamiltonian parameters $\boldsymbol{g}$ and D were known from powder spectra, the molecular orientation $\Theta = 29°$ in the single-crystal spectrum in Figure 14 could be determined from the resonance positions.

Triplet spin states give rise to two EPR transitions at each orientation of a molecule versus the magnetic field (see the X, Y and Z pairs of lines in Figures 13 and S4 and S6 in Supporting Information). The sign of D can be determined by measuring the relative intensity of the high-field and the low-field signal in such a pair at very high microwave frequency. If D is negative then the low-field line should be stronger than the high-field line at $\Theta < 60°$,[8] as is observed. The measured intensity ratio of 1.53 at 50 K is very close to the theoretical value of 1.50.[8] Similar relations were observed for **2**. Negative sign of D in dimeric perfluorinated copper carboxylates is therefore confirmed, and there is no reason to expect it to be positive in any other copper paddlewheel dimers. The sign of D plays a crucial role in estimating the anisotropic exchange-related contribution to the observed zero-field splitting,[8] and since most literature reports appear to be incorrect due to the assumption of a positive sign, we present some EPR parameters and recalculated $D_{exchange}$ data in Table 6.

The exchange-related part of D shows correlation with the electron-withdrawing strength of substituents in the carboxylate chain, and the increase in $D_{exchange}$ parallels the increase in the $\boldsymbol{g}$ components, as expected.[1,8,41−45] $D_{exchange}$ is related (through

(41) Morosin, B.; Hughes, R. C.; Soos, Z. G. *Acta Crystallogr.* **1975**, *B31*, 762–770.
(42) Muto, Y.; Nakashima, M.; Tokii, T.; Suzuki, I.; Ohba, S.; Steward, O. W.; Kato, M. *Bull. Chem. Soc. Jpn.* **2002**, *75*, 511–519.
(43) Ross, P. K.; Allendorf, M. D.; Solomon, E. I. *J. Am. Chem. Soc.* **1989**, *111*, 4009–4021.
(44) Ozarowski, A.; Reinen, D. *Inorg. Chem.* **1986**, *25*, 1704–1708.
(45) Gribnau, M. C. M.; Keijzers, C. P. *Inorg. Chem.* **1987**, *26*, 3413–3414.
(46) Brown, G. M.; Chidambaram, R. *Acta Crystallogr.* **1973**, *B29*, 2393–2403.
(47) Nakagawa, H.; Kani, Y.; Tsuchimoto, M.; Ohba, S.; Matsushima, H.; Tokii, T. *Acta Crystallogr. C* **2000**, *56*, 12–16.
(48) Pardi, L. A.; Krzystek, J.; Telser, J.; Brunel, L. C. *J. Magn. Reson.* **2000**, *146*, 375–378.

Table 6. Spin Hamiltonian Parameters for Dimeric Complexes

complex	g_x	g_y	g_z	10^4 D, cm^{-1}	10^4 E, cm^{-1}	r_{Cu-Cu}, Å	10^4 D_{dipole}, cm^{-1}	10^4 $D_{exchange}$, cm^{-1}
$[Cu(CH_3COO)_2H_2O]_2$ (80 K)[a]	2.0545(3)	2.0792(2)	2.3637(2)	−3350(10)	−103(1)	2.616[46]	−1710	−1640
$[Cu(CH_3COO)_2(pyr)]_2$ (80 K)[a,b]	2.0608(2)	2.0622(2)	2.3493(3)	−3280(10)	0(10)	2.58[41]	−1760	−1520
$[Cu(CF_3COO)_2(CH_3CN)]_2$ (80 K)	2.0709(2)	2.0752(2)	2.3905(3)	−4096(9)	0(10)	2.766[5]	−1610	−2490
$[Cu(CF_3COO)_2(quin)]_2$ (80 K)[c]	2.0836(3)	2.0836(3)	2.4115(4)	−4330(15)	0(10)	2.886[6]	−1440	−2890
$[Cu((CH_3)_3SiCH_2COO)_2]_n$ (280 K)[d,e]	2.0578(4)	2.0774(4)	2.3618(5)	−3188(17)	−83(9)	2.618[47]	−1860	−1328
$[Cu((CH_3)_3SiCH_2COO)_2(py)]_2$ (280 K)[e]	2.0699(5)	2.0699(5)	2.3697(6)	−3332(26)	0(20)	2.632[47]	−1840	−1490

[a] Spin Hamiltonian parameters from ref 8; all others are from this work and were determined from high-field EPR by global fitting of spectra recorded at 4 different frequencies, around 112, 224, 324, and 406 GHz. See also a note below Figure S2 in Supporting Information. [b] pyr: pyrazine; py: pyridine; quin: quinoline. [c] Significantly incorrect $g_x = g_y = 2.17$ reported in ref 6 illustrates difficulties in extracting spin Hamiltonian parameters from X-Band EPR, where $|D|$ is comparable to the microwave quantum energy. [d] The complex forms a chain of paddlewheel entities, but EPR spectra of isolated $S = 1$ state are observed. [e] Complex was prepared as described in ref 47 for comparative purposes, and no data other than EPR were collected. See Figure S6 in Supporting Information.

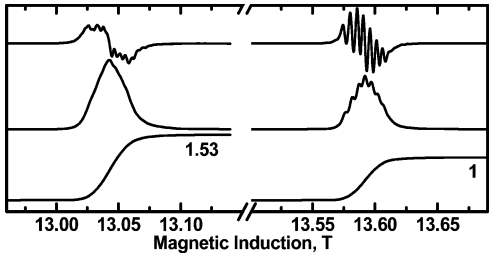

Figure 14. (Top) Single-crystal spectrum of **1** recorded at 50 K with $\nu =$ 432.0 GHz. (Center) Integrated signals. (Bottom) Doubly integrated signals. Signal integration was needed to extract the real intensity ratio of the low-field line to the high-field line (1.53) because the line widths are considerably different. The molecular orientation $\Theta = 29°$, meaning that the magnetic field lies 29° from the Cu−Cu direction, could be inferred from the resonance positions.

the spin−orbit coupling) to the exchange interactions in excited states of a dimeric molecule:

$$D_{\text{exchange}} = [J(x^2 - y^2, xy)\Delta_z^2 - 2J(x^2 - y^2, z)\Delta_y^2 - 2J(x^2 - y^2, yz)\Delta_x^2]/32 \quad (15)$$

where $\Delta_z = g_z - 2.0023$, etc., $J(x^2 - y^2,n)$ represent the triplet-singlet separations in excited dimer states in which one of the copper atoms is in its electronic ground state $d_{x^2-y^2}$, while another one is in an excited state n.[1,8,41−45] Increased magnitudes of both the $\boldsymbol{g}$ components and D_{exchange} in fluorocarboxylates compared to plain carboxylates reflect a reduced covalency of the $Cu-O_{\text{carboxylate}}$ bonds in the former ones.

Conclusions

Two new ferromagnetic and two antiferromagnetic (one of unknown structure) tetranuclear copper complexes were investigated by high-field EPR and magnetic susceptibility measurements. Broken symmetry DFT calculations were performed for tetramers of known structure to estimate the exchange integrals. Calculations correctly predicted the type of magnetism (ferro versus antiferro) in each of the three cases attempted. The calculated exchange integral magnitudes were in a semiquantitative agreement with the experimental data in both tetramers and dimers. Knowledge of the zero-field splitting parameters, which were determined from the high-field, high-frequency EPR, proved to be crucial for the interpretation of the lowest-temperature magnetic susceptibility and magnetization data for our ferromagnetic tetramers **3** and **4**. The dipolar contribution to the zfs parameters in **3** and **4** was found to be negligible, whereas it is of comparable magnitude to the exchange-induced zfs in copper paddlewheel dimers (Table 6 and ref 8). The copper(II)-trifluoroacetate-quinoline system is unusually rich with at least five different tetranuclear complexes known at this time (this work and ref 21), plus one binuclear compound.[6] In addition, at least one synthetic avenue leading to a nonmonomeric complex was abandoned in this work. This abundance of compounds is probably due to the possibility of formation of extensive hydrogen bond networks that stabilize various structures. Also, bonds between the carboxylate oxygen atoms and copper are weaker than in nonhalogenated carboxylate complexes providing additional flexibility to the system. Finally, negative sign of the zfs parameter D was found in binuclear acetonitrile and quinoline adducts of copper trifluoroacetate (**1** and **2**), and it is postulated that D is negative in all copper paddlewheel dimers.

Acknowledgment. This work was supported by the NHMFL, which is funded by the NSF through Cooperative Agreement No. DMR-0654118, the State of Florida, and the DOE and by the Ministry of Science and Higher Education of Poland through grant N204 049 31/1376. J.J. thanks the Wrocław University for support.

Supporting Information Available: CIF files for **2a**, **3**, and **4**. Scheme illustrating transformations of compounds studied in this work. Energy levels and EPR transitions in the $S = 2$ spin state of **3**. Resonance fields versus microwave frequency plot for **3** and note on parameter error estimation. Simulation of a high-field EPR spectrum of **4**. Solid-state conversion **2** ↔ **2a** followed by EPR. Exchange integral determination for **1** from magnetic susceptibility and EPR signal intensity. Experimental and simulated EPR spectra of $[Cu((CH_3)_3SiCH_2COO)_2]_n$ and $[Cu((CH_3)_3SiCH_2COO)_2(py)]_2$. ORTEP plot for **4**. Torsional angles and hydrogen bonds in **2a**, **3**, and **4** and stacking interactions in **3** and **4**. Shortened output of ORCA calculations. This material is available free of charge via the Internet at http://pubs.acs.org.

JA902695Y